Republic of Iraq
Ministry of Higher Education and
Scientific Reserch
University of Babylon
Collage of science for women
Department of Laser physics

Semi Plasmonic Core-Shell Nanomaterials as New Efficient Random Lasing Media

A Thesis

Submitted to the Council of the College of Sciences for Women at the University of Babylon in Partial Fulfillment of the Requirements for the degree of Master Science in Laser Physics

By
ZainabMajed Abdul Saheb

Supervisor
Dr.Saddam FlaeehHadawi
Dr.Read Naji ALI

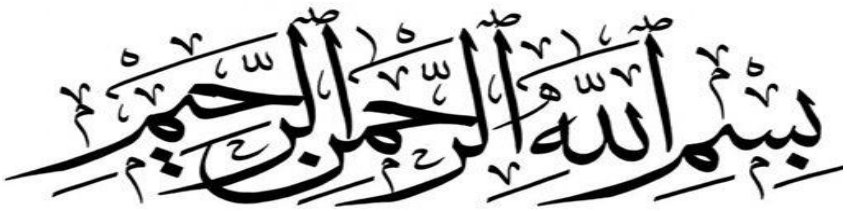

﴿ إِنَّ اللَّهَ وَمَلَائِكَتَهُ يُصَلُّونَ عَلَى النَّبِيِّ
يَا أَيُّهَا الَّذِينَ آمَنُوا صَلُّوا عَلَيْهِ وَسَلِّمُوا تَسْلِيماً ﴾

صَدَقَ اللهُ العلي العظيم

سورة الاحزاب/آية:(56)

Supervisors certificate

I certify that this thesis entitled" Semi Plasmonic Core-Shell Nanomaterials as New Efficient Random Lasing Media" by student(zainabmajed) under my supervision in the department of laser physics, college of scince for women, university of Babylon, as a partial fulfillment of requirement of the degree of master in laser physics

Signature
Dr. Saddam FlaeehHadawi
Assist Professor
Date: / / 2022

Signature
Dr. Read Naji ALI
Doctor
Date: / / 2022

Head of department certificate

In view of the available recommendation, I forward this dissertation for debate by the examining committee.

Signature
Name :dr. Jinan Ali Abd
Assist Professor
head of laser physical department

Address :
Date:

Dedication

To those with whom God guided us to the straight path, and to those who accepted us to be with them from among the survivors, and to those who raised for us the beacons of knowledge and guidance, and to those who brought us out of darkness into light, to the firmest handhold and the firm rope of God..... To my infallible masters and imams The fourteen - peace be upon them

To my first example, and my beacon that lights my path, to the one who gave me and continues to give me without limits, to the one who raised my head high in pride..... my dear father

May God keep him as an asset to me

To the one whose heart saw me before her eyes, and whose bowels embraced me before her hands, To my tree that never withers, To the shadow in which I shelter at all times..... My beloved mother

may God save her

To the most wonderful body of love in all its meanings, it was the bond and giving, and it gave me a lot in images of patience, hope and love..... My dear husband

To the candles that light the way for me and the source of my pride who encouraged me and continued to give without return my brothers and sisters.....

To the seed of the heart and the hope of tomorrow..... my children

To the luminous jewel, the preserved pearl, and the hidden pearl.... my dear daughter

Acknowledgement

Praise be to God as it should be for the majesty of his countenance and the greatness of his authority, the number of his creation, the contentment of himself, the weight of his throne and the ink of his words that it is upon me to accomplish this message, and prayers and peace be upon the best of creation, our Prophet Muhammad and his family and peace be upon him greatly.

I would like to extend my heartfelt thanks, gratitude, gratitude and utmost respect to my esteemed professor, Assist. Prof. Dr. Saddam FalihHedawi and. Dr. RiyadNaji, who are the supervisors of this thesis, who gave me a lot of their time and guidance and for the valuable information they gave me that contributed In enriching the subject of my study in its various aspects. I also extend my sincere thanks to the head of the Department of Laser Physics, Assist. Prof. Dr. Jinan Ali.

Abstract:

In this work, the effect of type scattering centers on the performance of random laser systems has been studied, in particular the intensity of their emission spectrum, the width of the emission spectrum (FWHM), and the laser threshold. The effect of the semiplasmonic nanoparticles concentration was studied, separately, and it appeared through the experiment that the appropriate concentration of the dye must be chosen and a specific range of the concentrations of nanoparticles within the dye, so the performance of the Al NPs random laser is studied at five different concentrations (500, 600, 700, 800 and 900Pulse) for each of them. It has been found that the greatest emission intensity in Al NPs (approximately 19000 a.u.), the lowest laser threshold (40μJ), and the lowest FWHM (12.5 nm) was obtained at the concentration of 800P. It was observed that these properties improved further by reaching the intensity of 21400 a.u., while the laser threshold and FWHM decreased to (35μJ) and (10.5 nm), respectively when the concentration became 800P in Mg Nps.Where, our results in core-shell NPs showed efficient coherent random lasing with Full width at half maximum(8.7)nm and peak intensity (27850 a.u.) with lower lasing threshold reach to (30μJ) for the sample with higher Mg shell thickness Al@Mg200P mixed with Rh6G due to the interface between two different semi-plasmonic nanoparticles in the middle part of the visible spectral region considering its applicability in the design and fabrication of compact and miniaturized random laser sources.

List of contents

List of Tables

List of Figures

List of Symbol

Symbol	Description	Unit
E	Electric field	V/m
$p\varepsilon$	Total charge density	$C.m^3$
B	Magnetic flux density	T
ε_0	Free space permittivity	F/m
μ_0	Free space permeability	H/m
J	Total current density	A/m^2
m_e	Electron mass	G
γ	Electron damping ratio	--
q_e	Electron change	Col.
ω	Angular frequency	Hz
P_a	Polari ability	$C.m^2/V$
D	Electric displacement	C/m^2
ε	Material permittivity	Hz
ε_d	Permittivity of surrounding medium	F/m
σ_{SCS}	Scattering cross section	m^2
σ_{aCS}	Absorption cross section	m^2
k	Wave number	m^{-1}
τ	Electron characterize time	ns
p	Density of material	g/m^3
R	Radius of nanoparticle	m
ε_{max}	LSPR peak frequency	Hz
n	Refractive index	--
λ_p	Wavelength plasma frequency	nm
λ_{max}	LSPR peak wavelength	nm
k_{med}	Thermal conductivity of medium	W/m.K
T^{cw}	Temperature generation due to cw irradiation	K
T^{pulsed}	Heat generation due to pulsed laser irradiation	K
I	Power density	W/m^2
R	Distance from center of nanoparticle	m

I°	**Incident irradiance**	**W/m^2**
V	**Volume of nanoparticle**	**m^3**
k_{sc}	**Coefficient of the scattering**	**W/m^2**
ℓ_{sc}	**Scattering mean free path**	**mm**
X	**Cuvette thickness**	**mm**
$I_{\circ}$	**Transmitted intensity through pure solvent without gain or scatteres**	**W/m^2**
$(\cos\theta)$	**Average cosine of the scattering angle**	**rad**
ℓ_t	**Transport mean free path**	**mm**

List of Abbreviation

Abbreviations	**Description**
NPs	Nanoparticles
AL	Aluminum
Mg	Magnesium
FWHM	Full widthat half Maximum
RL	Random Laser
LAL	Laser Ablation in liquid
Rt	Room Temperature
SPP	Surface Plasmon polartion
LSP	Localized surface plasmon
TEM	Transmission Electron Microscopy
SPR	Surface Plasmon Resonance
MNPs	Metallic nanopaticls
oD	Zero dimension
1D	One dimension
2D	Two dimension

الخلاصة

في هذا العمل ، تمت دراسة تاثير انواع مراكز التشتت على اداء انظمة الليزر العشوائية ، ولاسيما شدة طيف انبعاثها ، وعرض طيف الانبعاث(FWHM)،وعتبة الليزر . تمت دراسة تاثير تركيز الجسيمات النانوية شبه البلازمونية بشكل منفصل، وظهر من خلال التجربة انه يجب اختيار التركيز المحضر من الصبغة مع مدى محدد من تركيز الجسيمات النانوية مع الصبغة ، وبالتالي فان اداء الليزر العشوائيللالمنيوم(AL NPs) تمت دراسته من خلال خمسة تراكيز مختلفة للالمنيوم (P 500,600,700,800,900) لكل منهما . لقد وجد ان اكبر كثافة انبعاث في ALNPs حوالي19000)a.u، وادنى عتبة ليزر (40مايكرو جول) وادنى قيمة لاعظم عرض عند منتصف القمةFWHM (1205نانومتر) تم الحصول عليها عند التركيز(800 نبضة). وقد لوحظ ان هذه الخصائص تحسنت اكثر من خلال الوصول الى كثافة انبعاث(21400)، بينما انخفضت عتبة الليزر الى(35مايكروجول)وال FWHM الى (10.5نانومتر) عند التركيز (800نبضة) للمغنسيوم . اظهرت النتائج ليزر عشوائي متشاكه عند استخدام (اللب–قشرة) حيث كان اقصى عرض عند منتصف القمة FWHM(7.8نانومتر)وكثافة الانبعاث(27850) مع عتبة ليزراقل تصل الى(30مايكروجول) للعينة عندما يكون المغنيسيوم هو القشرة وذو سمك عالي.AL@Mg عند تركيز (200نبضة) عند مزجها مع الصبغة(RH6G)طبقا للسطح الفاصل بين اثنين من الجسيمات النانوية في الجزء الاوسط من مدى الطيف المرئي مع الاخذ بنظر الاعتبار قابليتها للتطبيق في تصميم وتصنيع مصادر الليزر العشوائية المدمجة والمصغرة

جمهورية العراق

وزارة التعليم العالي والبحث العلمي

جامعة بابل

كليــة العلــوم للبنـــات

قسم فيزياء الليزر

المواد الشبه البلازمونية المستخدمة كأوساطفعالةجديدة لليزر العشوائي

رسالة مقدمة الى

مجلس كلية العلوم للبنات-قسم فيزياء الليزر-جامعة بابل

وهي جزء من متطلبات نيل درجة الماجستير في العلوم فيزياء الليزر

من قبل

زينب ماجدعبدالصاحب

المشرف

ا م د صدام فليح حداوي

م د رياض ناجي علي

1444 هـ 2022 م

Chapter One

Introduction

1.1 Introduction

Many researchers in the past decade aroused research interest in many laser active media fields, and the brightest was in the random laser, where the theoretical studies conducted by the Russian scientist Letokhov on the light diffusion in random media indicate the possibility of light amplification by random scattering [1]. as The experimental studies have certain the significance of choosing nanoparticles inside active media that act as scattering centers due to their significant effect to enhance the gain which happening of this type of laser[2].The multiple scattering in the random active gain media system serves as a feedback mechanism for transfer to the stimulated emission of radiation [3].

The difference between the random laser and the conventional lasers is centered on the mechanism of confining the photon inside the active medium, the process of confining photons inside the active media in the random lasers by the multiple scattering in random systems, and this is done by nanoparticles, which act as a scattering center when added inside the random media [4, 5]. The light scattering phenomenon is obtained from disordered that happen in different active media such as dye-doped nematic liquid crystal [6], Semiconducting nanoparticles [7] Two-dimensional plasmonic random laser [8], organic dye-doped gel films [9], and so on. Since the properties of random lasers, including the peak intensity,line width, and lasing threshold can be influenced by multiple light scattering effects, size, type, and concentrations of nanoparticles [10].Depending on the type of nanoparticle within active media, random lasers can be transfer from incoherent (non-resonant) to coherent (resonant). In case of using plasmonic nanoparticles more quickly than by using nanoparticles do not have this phenomena. So the plasmonic nanoparticles are rich in the surface plasmon resonance phenomena

(SPR), which can be trapping of photons near the nanoparticles surface and leads to get random laser with high efficiency [11]. In the incoherent random laser, multiple scattering increases the paths of photons, thus, the feedback mechanism increases the photon lifetime in the active media. In the coherent random laser, the photon lifetime decreases and returns to its first position forming a closed path [12].The plasmonic nanoparticles mixed with dye have Stokes shifts between their absorption and emissions, which can reduce self-absorption and lead to enhancing the threshold with low energy pumping [13]. The emission spectrum can be enhanced with the assistance of a plasmonic by coupling between the dye and LSPR of a plasmonic nanoparticle [14]. We will study the effect of two types of nanoparticles (Al and Mg NPs) and each type with five different concentrations, and the range of the impact of each parameter will be studied on the properties of the random gain media to choose the suitable medium for the random laser system. These parameters will be discussed and their effect on the peak intensity, full width at half maximum (FWHM), lasing threshold, and the number of spikes as well as their impact on other factors such as scattering mean free path (l_s) and transport mean free path(l_t). Which can be considered as the basic factors for understanding random laser behavior.Reducing the price of the gain media and reduction of the pump power as low as possible is still an open question. For this reason, new types of gain media were introduced, including the above-mentioned NPs but in a new mixture or core-shell form. The effect of NPs' interface in the core-shell structure plays an important role to change their absorption and mainly scattering to achieve coherent lasing. Similarly, one may know that for semi-plasmonic NPs in the core-shell form, an efficient overlap and adjustable/ tunable SPR wavelength takes place by changing the shell thickness, the effective volume of the main core, and the host medium of the NPs.

1.2 Applications of random laser

The simple structure of random laser, less cost of fabrication, the ability of operation at a specific wavelength which covers a wide range of regions of the electromagnetic spectrum, make the random laser is the best than any of normal lasers in many applications fields such as industrial[96], commercial[97], and medical [98]. The random laser has the only a disadvantage; it is pumped by external laser to cause excitation and emission.

The random laser used in the photonic barcode, has a narrow line width emission signature, makes it perfect for producing wavelength-domain photonic codes, which can be recognized in long-range or short-range. In short-range applications, one can think of photonic bar codes for documents [99]. Long-range such as military applications [100].

Random lasers also used in manufacturing optically homogeneous optical diode; it has widely used in electronics fields to follow the current in one direction [101].

Random lasers can also be used in biological and medical studies. When the nanoparticle clusters are attached to biological targets, the position of the targets can be tracked by detecting the lasing emission from the clusters. We can differentiate the targets because each nanoparticle cluster has its own unique set of lasing frequencies [93].

1.3 Literature Review

Since a few years ago, the plasmonic random laser study has been studied. Due to its significance in numerous application domains, there is an urgent need for additional research. A few of them are shown in the paragraphs that follow.

In 2010Murai, Shunsuke, et al. [15]. Focusing on the noble NPs' scattering properties, one of the standout lines connected to localized surface Plasmon resonance, and showing how they are used as parts of a cavity random laser, we affirm the benefits of metallic NPs' scatterers over those in dielectric NPs by highlighting an example.

In 2011 Xiangeng. M, et al [16] reported and experimentally tested By modifying the coupling between photons and surface plasmons in lasing media made of organic dyes and metallic-dielectric core-shell nanoparticles, the capability to control random lasing resonance features. When the strength of scattering is low enough, it is found that based systems-core shell nanoparticles exhibit optical feedback characteristics that set them apart from media with pure metallic nanoparticles. The pump threshold rises with increasing shell thickness. It could demonstrate how crucial a part the local-field augmentation plays in the coherent feedback.

In 2012 ZnOLin, Ming C., etal[17] have been found thin films were created by employing atomic layer deposition over a SiO2 layer on a silicon substrate and quick heat annealing. ZnO thin films on SiO2/Si substrates to exhibit low threshold lasing. The stimulated emission random lasing shifted to the blue wavelength and increased the threshold random lasing with an increase in post-annealing period or decrease in ZnO film thickness.

.In 2013, Qiao, Qian, et al [18] study the random lasing capabilities used electrically pumped in Au/MgO/ZnO nanostructures to. The lasing threshold in these structures decreased from 63 mA to 21 mA by combining Ag NPs, whose extinction spectrum overlaps with the intensity random lasing well. The decrease in lasing threshold can be attributed to the Ag NPs' surface plasmon and the resonant coupling between the carriers in the structures' active layer.

In 2014 Ismail, Wan Z., et al. [19] , investigated the signatures of spectral and coherence random lasing threshold with incoherent optical feedback Using alumina colloidal NPs suspended in Rh6G dye and pumping by nanosecond laser. The feedback in this medium was provided by multiple scattering from the alumina particles. They investigated the diffusive scattering regimes and discovered that scattering length and nanoparticle concentration had an impact on weakly scattering. At the lasing threshold, an abrupt increase in peak strength and a fall in the FWHM of a single dominant emission peak coincided with a sharp increase in the clarity of the interference fringes.

In 2015 Ziegler, Johannes, et al [20].StadyRandom lasing gold nanostars were shown to act as scattering centers in the Rh6G doped gain medium by The gold nanostar has been demonstrated through experimentation to be superior to a spherical shape. They created the gain medium in the form of thin films to create resonators that improve coherent random laser modes. They selected gold nanostars because they have enhanced by high plasmonic field, localized at the spiky tips, and the sample excitation by single-pulsed, the FWHM in this medium appeared less than 0.2 nm, and random lasing threshold 0.9 cm2.

In 2016, Zhai, Tianrui, and colleagues [21] achieved a Dual-wavelength laser emission in a sandwich structure that was active/inactive/active. The active and inactive layers are made of poly [(9, 9-dioctylfluorenyl-2, 7-diyl)-alt-co-(1, 4-benzo-(2, 1 0, 3) -thiadiazole)] and polyvinyl alcohol, respectively. Dual wavelength random lasing is seen simultaneously and is attributed to the two active waveguides' various refractive indices. Designing small laser sources is flexible thanks to the sandwich structure.

In 2017 Xiangeng, Koji, et al. [22]. were studied by gathering the samples' back emission The random lasing properties by localization transition in a very disordered scattering gain medium imperturbable of core/shell NPs TiO2@Silica in Rh6G dye solvent in ethanol solution, they measured the fluorescence band independently. However, frontal emission collection revealed that the absorption and emission spectra were saturated. They noticed very intense peaks right above the superfluorescence band. When compared to the passive modes of the scattering gain medium, these peaks have a narrower line width.

In 2018 Lü, Hao, and et al. [23].focased on the dye-doped polymer with dispersed Au NPs (DP@Au NPs) to improve plasmonic random lasing was reported by A DCJTB-doped PMMA film contains scatterers made from heat annealed Au NPs and easy sputtering techniques. With the annealing temperature and sputtering time optimized, Au NPs with random arrangement were created. In random lasing emissions via multiple scattering, the particles are crucial. By demonstrating polarization dependency and low-threshold random lasing in the DP@Au NP system, we observe random lasing emission as a function of detection polarization and pump beam strength.

In 2019, Zhang, Shuai, et al. [24] modified the cavity coupling to manage the distributed feedback polymer random laser's threshold and polarization. Two gratings were used in the distributed feedback polymer random laser's cavity structure, which was created utilizing a two-beam multi-exposure holographic technique. Tuned coupling strength of the cavity modes is achieved by adjusting the angle between the two gratings. At the lowest coupling strength recorded minimum random lasing threshold, the threshold random lasing decreased with decreasing the coupling strength of the cavity modes. Azimuthally polarized polymer laser power has also been altered by altering the cavity coupling.

In 2019Choi, Dongsun, and Kwang S. Jeongi.[25] shown Tellurium microcrystals and bulk crystal's photoluminescence and random lasing capabilities. Spotted the tellurium bulk crystal's photoluminescence at 3.75 m in the mid-infrared spectrum. This outcome is compatible with the theoretical part. At 3.62 m, the photoexcitation intensity of the bulk Tellurium crystals was seen to randomly vary as the temperature changed. Rod-shaped Tellurium microcrystals display second harmonic and third harmonic lasing with high efficiency in the mid-wavelength and short-wavelength infrared regions, respectively. Tellurium microcrystals will produce a nonlinear coherent mid-infrared random laser that will be an outstanding source of middle-infrared light

In 2018, JiajiaYinl and colleagues[26] investigated how the size of nanoparticles affected a system of random lasers. They created three samples: S1 comprises R6G with Au nanorods that are 40 nm in diameter and 68 nm in length; S2 is R6G with Au nanorods that are 40 nm in diameter and 84 nm in length; and S3 is R6G with Au nanorods (diameter 40 2 nm, length 96 2 nm). R6G and Au concentrations were both fixed. The greatest length medium, according to experience, provides a lower

lasing threshold. As a result, many discrete narrow laser spikes with FWHM less than 1 nm arise in the emission spectra when the pump energy reaches its threshold (blue lines in the three photos)

In 2019ibyZhiRen et al.[27], investigated how the wavelength-tunable random laser was also createdand film was built utilizing R6G, PVP, and Au NRs using a silicon rubber slab as a substrate. This silicon panel has a fantastic mechanical elongation capability. The core wavelength of the laser output shifts toward shorter wavelengths (blue shift) from 592 to 585 when the stretching amount increases from 0 to 12 mm. Additionally, the surface plasma resonance provided by the gold nanoparticles significantly boosts the amount of light that the dye molecules can absorb. As a result, the dye molecules' fluorescence should be significantly boosted, which might result in a drop in the random laser threshold of roughly 9.8 mJ/cm2. The FWHM drops from 40 nm to 3 nm at the threshold. A detailed illustration of what was discussed previously

In 2020, V. S. Gummaluri and colleagues [28].were successful in creating a random laser system using gold nano-urchins scattered across a rhodamine 6G dye-doped polymer screen as scatterers. They contrasted it with another device that met the same parameters, but used gold nanospheres as the scatterer rather than gold nano-urchine. Utilizing finite-difference time-domain (FDTD) simulation, they examined the local field enhancement, absorption cross-section, and scattering cross-section in order to assess lasing performance. They noticed that the urchin's field intensity magnitude.

sphere twice that of. Additionally, they observed that at the pump wavelength, nano-urchins had a lower absorption cross-section and a higher scattering cross-section than nanospheres. This suggests that nano-urchins are more suitable scatterer candidates for improved random lasing performance than isotropic spheres

1.4 Aims of the Work

1- To achieve a random laser in the visible region, Al or Mg NPs with different concentrations in Rhodamine 6G (R6G) will be used.

2- introducing a new type of gain medium including the NPs as mentioned above but in a new core-shell form.

3- Producing these different concentrations of NPs mainly by laser ablation in liquid (LAL) method and investigating the effect of the interface and the thickness of the shell and the core-shell type in the double semi-plasmonic NPs as scattering points in the gain media. For this purpose, Al and Mg NPs were produced in different styles as core-shell and their mixture Rh6G media, which can open new insight into the plasmonic random laser field.

Chapter Two

Theory Part

2.1 Introduction

In the experimental part, we prepared different kinds of NPs, which represent scattering centers suspended in dye as a gain medium of our random laser. Two types of core-shell had been prepared in differentconcetration.. The laser ablation technique is used to produce different types of nanoparticles. Also, many measurement devices are employed in this work such as UV-Visible, transmission electron microscopy (TEM).

2.2 plasmonic

Plasmonics is the field of studycalled the optical phenomena that resulted from the interaction of electromagnetic waves with conduction free electrons of noble metal nanoparticles such as AuNPs, AgNPs, and PtNPs. Collective oscillation called as surface plasmon, by these types of nanoparticles can be reached to strong absorption due to the transitions between electronic bands [29].

Plasmonics forms a significant part of the enchanting field of nanophotonics, which can confine the electromagnetic field smaller than the wavelength. The enhanced optical near field of subwavelength dimension based on the interaction between (the electromagnetic field and conduction electrons at metallic interfaces) [30].

When incident electromagnetic fields on a noble metal surface, it will accelerate electrons and lead to induce polarization that creates restoring force which causes .an oscillation of the free electron of the noble metal as shown in figure (2.1). This oscillation is quantized and free electrons oscillation is a quantization of plasma oscillations, and it's called a plasmon [31]. The frequency or particular wavelength of the incident

light in this phenomenonis strongly dependent on the type, shape, size, and surface of noble metal nanoparticle [32].

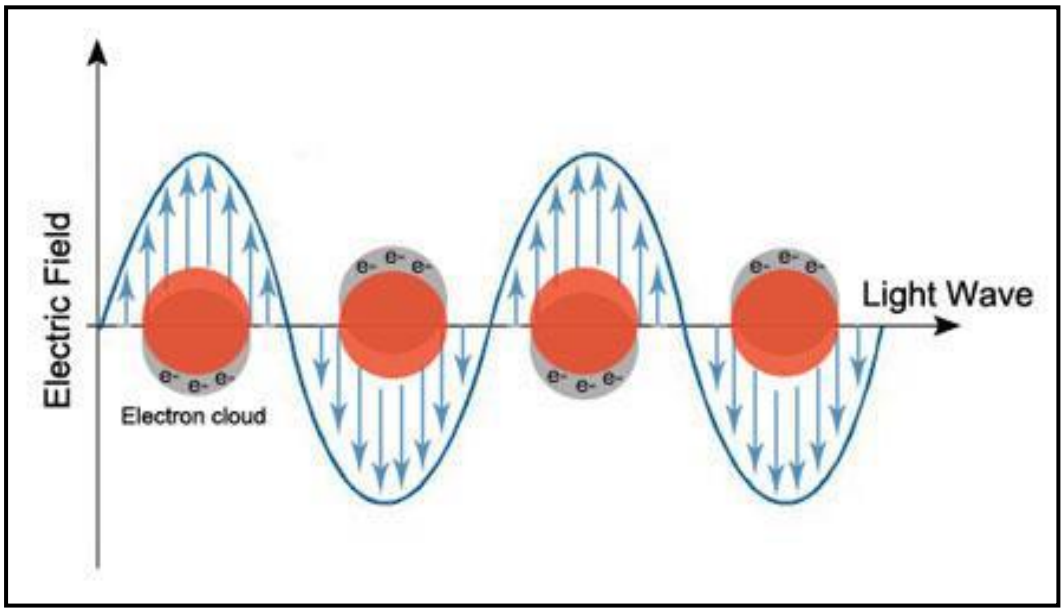

Fig. 2.1 Schematic describing surface plasmon resonance of metallic nanoparticle[33]

Surface plasmon divided into two types according to their interface: Surface Plasmon Polariton (SPP) and localized surface plasmon (LSP). SPP are longitudinal waves, which propagate at the interface between a metal and dielectric. These waves travel parallel to the direction of propagation in other words they cannot be excited by a transverse wave. The best way to excite a plasmon is, to use electrons, i.e. when light excites the electrons electrons will pass through thin metal, layer and lose some energy, and its use to excite SPP [33].

LSP is non-propagating waves. In the case of a spherical noble metal of nanoparticle, the curved surface of the noble metal of nanoparticle creates a restoring force on the electrons to result in a localized resonance. This type of resonance can be excited by incident electromagnetic field

directly on the surface [34]. LSP has two significant effects. First, electric fields near the particle's surface are greatly enhanced this enhancement being highest at the surface, and rapidly falling off with distance. Second, the particle's optical extinction has a maximum at, the plasmon resonant frequency, which occurs

at visible wavelengths for noble metal nanoparticles. This extinction peak depends on the refractive, index of the surrounding medium [35].

The interaction of noble metal nanostructures with electromagnetic fields can be understood in a classical framework based on Maxwell's equations. Even noble metal nanostructures with small size at a few, nanometers can be described without used quantum mechanics. Maxwell's equations depict the electromagnetic field for a given system during the four-vector force of the electric field (E), the strength of the magnetic field (H), the displacement (D), and the flux density (B) [36].

$$\nabla . \vec{E} = \rho e \varepsilon 0 \qquad (1\text{-}1)$$

$$\nabla . \vec{B} = 0 \qquad (1\text{-}2)$$

$$\nabla \times \vec{E} = - \partial \vec{B} / \partial t \qquad (1\text{-}3)$$

$$\nabla \times \vec{B} = \mu 0 \ \varepsilon 0 \partial \vec{E} / \partial t + \mu 0 \ J \qquad (1\text{-}4)$$

Where ρe is the total charge density), J is the total current density, and $\mu 0$, $\varepsilon 0$ are the permeability and the permittivity of free space.

The incident external electric field excites the free electrons and displaces it from their normal positions in the metal lattice. Movement of the oscillating free electron can be described by the equation of motion[37]

$$me\ x..+me\gamma\ x.=-qeE \qquad (1\text{-}5)$$

Where E is the external electric field, qe is the electron charge, me is the free electron mass, γ is an electron damping factor, and x is the electron displacement.

2.3Rhodamine 6G Laser Dye

The Rhodamine 6G has a broad range of frequencies, including the orange light frequency of 590 nm, where its pumping green laser source 532 nm. The molecular formula of this dye $C28H31N2O3\ CI$ and 479.02 g/mol molecular weight. Rhodamine 6G has highly efficient [38], and it has Rhodamine high quantum efficiency, where the quantum efficiency is the significant parameter in determining the random lasing properties [39].

Rhodamine 6G can be used as pigments and as fluorescent probes to describe the surface of polymer nanoparticles, studies of the structure of molecules, and the one of the most important used as an active medium in random laser due to its high fluorescence quantum yield [40,41] In addition to other uses [42,43]. The chemical structure of a Rhodamine 6G dye shown in Figure. (2-2).

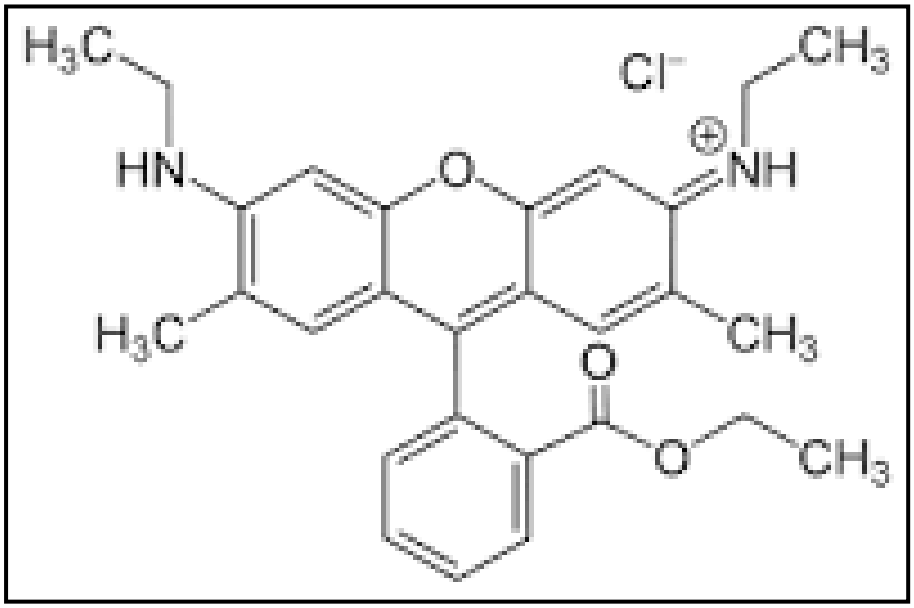

Fig. (2.2) the molecular structure of Rhodamine B laser dye.[43]

2.4 Scattering

Scattering is defined as the process in which the direction of propagation of incident light changes and occurs when this light collides with an obstacle [44]. The charges in the atoms or molecules of the scattering particles will respond to incident light, and the electric vector of this light will shift and thus reorienting the charges producing a microscopic dipole. This dipole will emitlight of the same frequency, in all directions barring the one along the polarization axes [45]. The energy of the incident light is higher than the energy of the scattered light in all directions. The intensity of the scattering filed depends on the scattering angle and frequency of the incident light.

When the wavelength of the incident light is greater than the size of scattered $x<<\lambda$, the scattering, in this case, was named as Rayleigh scattering [46]. When the scattering is the same in both backward and forward directions, its cross-section in this case, and depends on the wavelength of the light and scatterer size. Furthermore, Mie scattering takes place at particle size is nearly equal to the light wavelength. The intensity of the scattering is more in the forward direction, and the cross-section is greater [47]. Thus, the particle size compared to incident light specifies which one of Rayleigh and Mie scattering may occur, and can show the difference between them in the figure. (2-3)

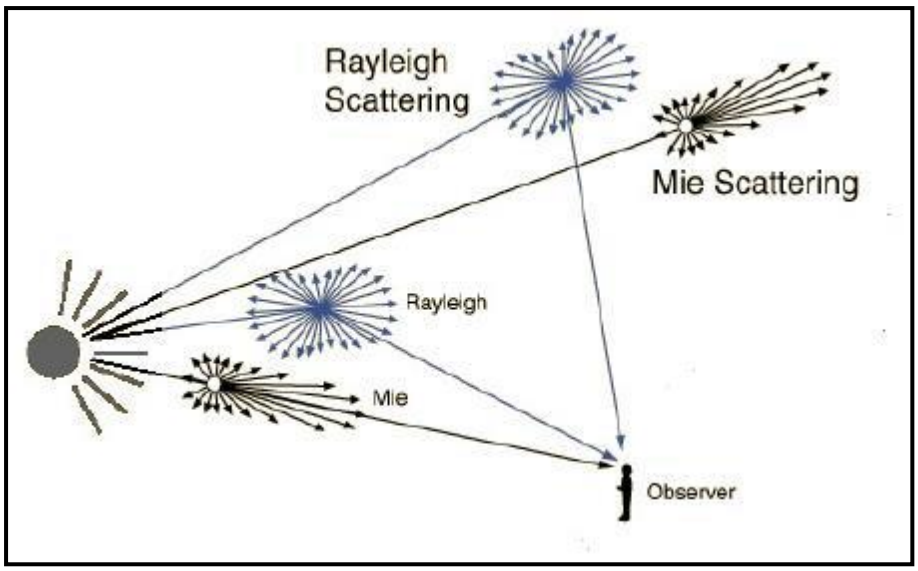

Fig. (2-3) The difference between the Rayleigh and Mie scattering [48].

2.4.1 Single Light Scattering

The single scattering is the scattering occurring due to atom or molecule, and the scattering of light from one scatter only. In single scattering, the media seems random to a viewer because no relation found between the direction of income and outcome light [49]. When the scatterers are randomly distributed and are separated from each other by a distance greater than their size. The incident light on the single-particle, induced firstly an electric polarization inside the particle. A new electromagnetic wave was created around the scatter and inside it due to that polarization. The total electromagnetic wave induced polarization in the scatter [50]. Each particle scatters light separately, and there is no constant phase relationship between the scattered waves. When the concentration of scatterers is low, this type of scattering the probability of occurrence is high in the medium [51]. Then, the photon mean free path in this medium is long, can be enhanced photon mean free path by increasing the concentration inside the medium, which increases scattering, to get a coherence random laser.

2.4. 2 Multiple Light Scattering

The scattering varies with the average radius of particles, incident wavelength, scattered density, index of refraction [52]. The scattering in all directions occurs if the size of particles is smaller than the incident wavelength ($\lambda << Z$), the light may be scattered many times within its propagation through the scatters and this kind of scattering is called multiple scattering [53]. The scattered light inside the medium has a random path; also the light in this type of scatters has a path longer than the rectum path of the waves, so the waves leave medium without scattering [54,55].

The random laser action is related to multiple scattering by the introduction of a disturbance inside a random laser gain medium, and this medium should be homogeneous, and small particle size, high refractive index, and low absorption at the excitation wavelength [56]. Multiple scattering provides the optical feedback mechanism; this the scattering density is the great interface between the gain of the active material and multiply scattered waves. Thus it can access to significant light amplification. The interference has the most significant effect on the multiple scattering than single scattering because of a large number of scattered arrays from different scatters [57].

2.5Length Scales in scattering Random Media

It is difficult to indicate significant characteristics of random laser because this domain has not been studied long, the operation mechanism of random laser remains not clear, the structure of the disordered medium is very diverse, *etc*. However, we can reveal some apparent characteristics. To understand random laser, there are two very important parameters: scattering mean free path and transport mean free path.

2.5.1 Scattering mean free path (ℓsc)

The scattering mean free path is defined as, the average distance that light travels between two consecutive scattering events [58]. Two quantities determine the magnitude of the effect on the light: the strength of the scattering of one particle with the filed, and the number of particles. The former is quantified as the cross-section σsc, and the latter is the particle densit$n$ [59,60].

$$\boldsymbol{k_{SC} = n\sigma_{SC}\ or\ its\ inverse\ \ell_{SC} = \frac{1}{n\sigma_{SC}}} \qquad (\mathbf{1-6})$$

Where κsc is the coefficient of the scattering and has a dimension of inverse length.

To reach a random laser condition, the varying density of nanoparticles was mixed with a dye solution. Change in scattering mean free path of the gainmedia for different concentrations of nanoparticles was estimated using the following approach [61].

$$\boldsymbol{\ell_{SC} = \frac{X}{\ln(\frac{I_0}{I})}} \qquad (\mathbf{1-7})$$

Where X is the cuvette thickness, $I0$ is transmitted intensity through pure solvent without gain or scatterers, and I is transmitted intensity of solvent suspended with particles.

The regime of multiple scattering occurs when $\ell sc \ll L$ but this regime no longer holds due to the multiple scattering can reintroduce the scattering light in the direction of the incident beam. Nevertheless ℓsc will be larger than wavelength [62].

If the material extreme scattering, with $\ell sc < L$, interface needs to be taken to account even after ensemble averaging due to the energy transport by this wave filed is affected [63].

For the case of $\ell sc<$, then the recurrent for scattered photons and increasing incoherent feedback will be achieved. The effect of ℓsc on the scattering strength k was showed in the following form [55]:

$$\boldsymbol{K\,\ell_{SC} = \left(\frac{2\pi}{\lambda}\right)\ell_{SC}} \qquad (\mathbf{1-8})$$

When $K\ \ell sc$ becomes smaller or equals to 1 , then $K\ \ell sc\leq 1$ (Ioffe –Regel criterion) or $K\ \ell sc\cong\lambda$ then the light propagation transfers to localization [64].

2.5.2 transport mean free path ($\boldsymbol{\ell t}$)

Transport mean free path can be thought of as the mean distance after a photon's direction becomes random. In other words the length, after which the light has lost its initial direction completely [65]. The transport mean free path has the following form:

$$\boldsymbol{\ell_t = \frac{1}{1-(\cos\theta)}.\frac{1}{n\sigma_{SC}}} \quad (\mathbf{1-9})$$

Where is the $\langle \boldsymbol{cos\theta}\rangle$ average cosine of the scattering angle, by using eq.1.6 we get:

$$\boldsymbol{\ell_t = \frac{\ell_{SC}}{1-(\cos\theta)}} \ (\mathbf{1-10})$$

when$\langle cos\theta\rangle$=0 , ℓt=ℓsc in this case Rayleigh scattering occurs, and when$\langle cos\theta\rangle$=0.5, ℓt=2ℓsc , so Mie scattering occurs in this case [66].

Transport mean free path is the important length scale, for the diffusion of the intensity. Where $\ell t\ll$, we are interested in the regime, so the light transport is truly diffusive. Since the propagation of the transparent mean free path is random, there is a net flow of light only if there is no uniform density; otherwise all microscopic propagation cancels [67].

2.6 Phenomenology

. Phenomenology stands in contrast with experimentation in the scientificmethod, in which the goal of the experiment is to test a scientific hypothesis instead of making predictions

2.6.1 Laser Threshold

The laser threshold is a very important factor of random lasing, and the threshold depends on the luminescence efficiency of the gain media, and the scattering mean free path of photons in the random media [68]. The lasing threshold reduced when the scattering mean free path is equal to or less than

the stimulated emission wavelength [69]. The concentration of scatters can influence the threshold when increased the concentration of the scattering particles, the lasing threshold decreasing [70]. The lasing threshold also depends on the refractive index of the scatters compared to that of the surrounding media, and is reduced when the refractive index of the scatters is increased or the refractive index of surrounding media is decreased [71]. In random laser to reduce the lasing threshold, used metal nanoparticles as the scatter, by these nanoparticles can induce surface plasmon resonance, and spatially confine the light near the surface to enable high gain. The metal nanoparticles have large scattering cross-section [72].

When the pumping the sample with low power is less than the lasing threshold and appeared single peak for spontaneous emission when increasing pump power, the emission decay time decreases quickly. Many spikes appeared, when increased pump power due to the existing large number of modes [73].

2.6.2 Reabsorption

Is the absorption of the emitted photons at other times by the same medium which is emitted from it, thus it probably happened after spontaneous emission, and it causes redshift, or after laser emission, where $\ell_{sc} > \lambda$, and emitted coherent photons are reabsorbed from un pumped molecules in the medium. This process can be represented as feedback for non-excited medium parts [74].

The redshift is caused by the absorption of the blue part, of the fluorescence by ground state dye molecules. The blue part of the spectrum is absorbed and re-emitted in a frequency distribution that is the spontaneous emission spectrum, which on average, is redder than the reabsorbed light [75,76].

2.7 Random gain media

Light travels in a vacuum with straight lines, while it has many variable directions, when light travels through a medium consisting of many particles (atoms or molecules) [77]. The propagation of light through a medium is controlled by the interactions between light and the matter, which is the main reason to change the direction of light in a medium [78]. The continuously changing of the propagation direction and the straight traveling is due to the scattering [79].

In recent years many researchers attracted an interest in improving the active medium of the dye laser. The first attempts started in 1960 and continue until now. It involves utilizing a polymer solution that contains organic dyes to form laser dye active media [80].

The dye utilized as a host of the active media is mostly in the liquid phase. This active media has many disadvantages and not easy to control. Therefore, it is best to mix it with a solid host, like polymers glass, to get a solid active medium. The dye laser used in the solid phase has a low

resistance of the polymer host to damage caused by the laser, so the dye laser in this style was limited in the past. It can be overcome to these defects by configuring the solidity of the polymer host through controlling the cross-linking with monomer then merging the active dye molecules leading to attain laser efficiency [81].

2.8 Random laser

In 1968 Letokhov prophesied that light amplification is possible in a random medium. In a random laser, the mirrors of a conventional laser are replaced by many small nanoparticles [82]. The random laser can be observed in disordered gain media, including disordered solutions, semiconductorpowder, nanostructured thin films, and so on [3]. It is distinguished by being an open resonator, in other words, it doesn't want an external cavity, and the feedback mechanism is provided utilizing the so-called scattering [83]. Based on some advantages that random laser owns, it has been studied widely and deeply in a recent couple of years. The random laser can bring people great benefits owing to the low cost, multidirectional light, changeable shape, and small size. It deserves to be studied, and it will change many application areas [84].

The incident light beam on the disordered medium can experience three possible processes: absorption, transmission, and reflection, which depend on the size of nanoparticles, the density of the gain medium, and intensity of the incident light [12,13]. The high density of scatterers, interference between waves occurs when there is a high density of scatterers. If the density of the medium is high or the size of nanoparticles is large, the photon experiences multiple scattering before leaving the medium, multiple scattering a significant phenomenon to backscattering [85]. Since the transferring waves are entirely on the same distance, they preserve the same primary phase relationship even though a large number

of scattering events forms the path. If the scattered waves are in a phase with each other, it occurs constructive interference and thus creating closed paths of light in the scattering media, as shown in figure (2-4) [86]. These close paths provide the feedback mechanism [87].

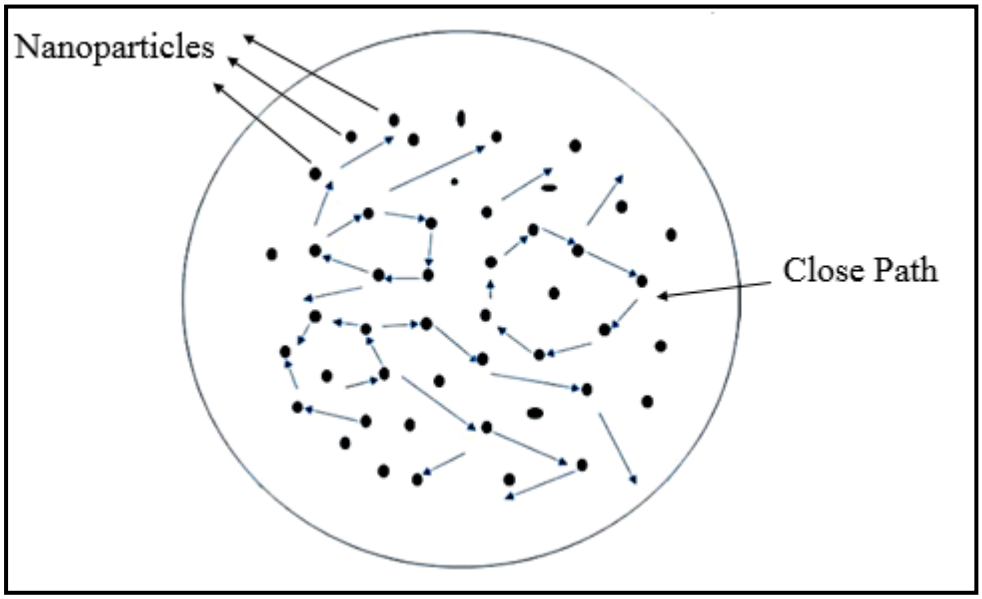

Fig. (2.4) random light path forming close loops in multiple-scattering media[87]

Based on the excitation of the random amplification media, the gain increases and overrides the loss [88]. The intensity rises very fast, yielding a strong pulse in different directions. With high intensity, the population inversion is emptied very fast, resulting in a short sharp peak in the emission spectrum. Thus, narrow emission peak emerges with a series of spike within the emission spectrum, therefore reduced a full-width at half-maximum (FWHM) with a high degree of temporal and spatial coherence [89]. The scattering inside the gain media contribute in trapping light photons due to multiple scattering, to do that, the light path inside gain media will be long time interval, and this is one reason to reduce the lasing threshold [90].

2.9 Types of Random laser

Which cases there aretwo random laser mechanisms: in-coherent random laser and coherent feedback random laser.

2.9.1 Incoherent feedback

It corresponds to incoherent lasing. The photon travels in a scattering medium and experiences a relatively long lifetime. Then it escapes the medium. There is enough time to get amplification, but no loop formed in this process [91]. So we can only observe a curve without sharp spikes. Light scattering mean free path is much longer than the emission wavelength. This belongs to a weakly scattering regime and results in an increased photon lifetime within the active medium [92].

2.9.2 Coherent feedback

Photons generate some closed-loop among different scattering centers when they propagate in a scattering medium. So some sharp spikes are shown [81]. The mean free path of light is close to the emission wavelength and results in localization of the radiation field in the medium [93]. This is characterized by a strongly scattering regime, and above a threshold, the emission intensity increases dramatically with discrete laser modes appearing in the emission spectrum

Thus, the expected difference between incoherent and coherent random laser is a sharp spike, which is caused by a close-loop light path in random media. Figure. (2-5) illustrates the formation of coherent and incoherent feedback in the gain medium [94].

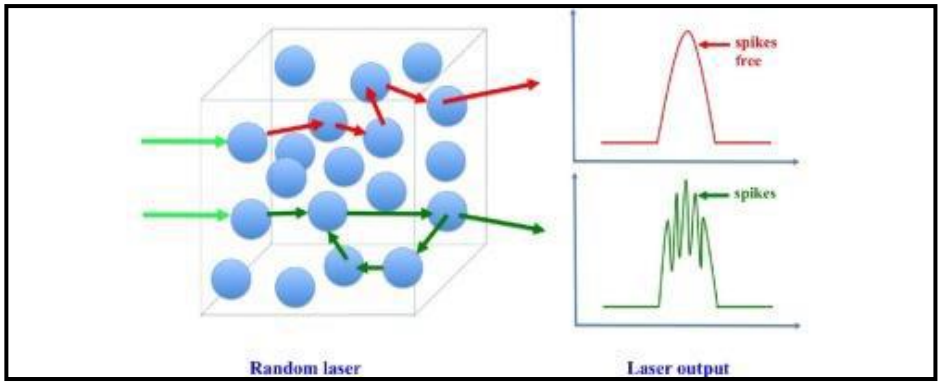

Fig. (2.5) represents the difference between the incoherent and coherent random laser in the gain medium[95]

From the figure shown, incoherent random laser, coherent random laser, and the transition between these two cases are all characterized. When the scattering is weak, under the same circumstance of dye concentration, photons propagate in scattering media, but difficult to form a closed loop. One photon generates another photons and the number of the photon increases. Thus the intensity of emission spectra is increasing suddenly. While the scattering is strong, the path of a photon can generate a closed-loop. This closed loop is like a resonant cavity in a conventional laser. Consequently, some sharp spikes are shown in the spectra [95].

2.10 Nanostructure

Nanoparticles of different types and materials at the range (1-100 nm), this scale provide many advantages, depending upon the size, shape, structure, and method of preparation [102]. Nanoparticles classified to 0D, 1D, and 2D NPs according to the agglomeration of atoms and molecules [103].

The agglomeration of nanoparticles depends on several factors, such as the type of nanoparticles, conditions of synthesis method, and concentration of nanoparticles in the solvent. By several processes can be avoided the agglomeration of nanoparticles, such as coating the nanoparticle surface by another organic or inorganic substance or

chemically stabilization [104]. Additionally, nanostructures divided based on single or multiple materials into simple and composite nanoparticles. Simple nanostructures are madefrom a single material. While composite nanostructures are made out of at least two materials, for example, core-shell nanoparticles [105,106].

2.10.1 Al nanoparticles

Aluminum (Al) nanoparticles have unique optical, physical, and chemical properties that make them candidates for use in a variety of applications, ranging from nanophotonics and catalysis to the preparation of high-energy composites. Through precise control of the synthetic process, nanocomposite has the ability to fabricate a variety of shapes and sizes and optimize plasmonic properties for your application. Below are just some examples of the diversity of aluminum nanoparticle configurations achievable at nanocomposite—including nanospheres, silica-shelled nanocubes, and faceted nanoparticles [107]. Aluminum nanoparticles are novel plasmonic materials with optical properties that extend into the UV, making them distinct from gold and silver nanoparticles that have plasmonic properties in the visible and NIR [108]. Control of the shape and crystal structure of aluminum nanoparticles thereby enables fundamental investigations in UV plasmonics and nanophotonics. Directing the shape of aluminum nanoparticles toward cube and concave-cube morphologies enables light energy to be concentrated onto the sharp corners and tips of the particles, creating strong localized field enhancements that are useful for sensing and photocatalysis. The surface oxide imparts unique functionality in sensing applications and is a built-in dielectric spacer for studying and utilizing plasmon-enhanced phenomena [109].

Properties	Numerical Factor
Atomic number (Z)	13
Massnumber (A)	27
Gram atomic weight (g)	26.98
atomic radius (A°)	1.43
Volumetric mass (g/cm^3)	2.7
Melting point (C°)	660
boiling temperature (C°)	2450
The first ionization energy (kg/mol)	0.578
Electron energy (e.v)	0.6

2.10.2 Mg nanoparticles

Magnesium is strong and light in its pure form. Hence it can be used for several high-volume manufacturing applications including in aerospace and automobile components. It tarnishes slightly when exposed to air and reacts with water at room temperature [110]. Magnesium nanoparticles are spherical black high surface area particles typically 20-60 nm in size with specific surface area ranging from 30 to 70 m2/g. These nanoparticles are also available in ultra-high purity, high purity, coated, and dispersed forms. Magnesium nanoparticles can be prepared using a number of methods. However, the production of magnesium nanoparticles through a mechanical milling process has been found to be an efficient method of producing magnesium nanoparticles [111]. The key applications of magnesium nanoparticles such as automobiles and airplanes, coatings, nanowires, plastics, and nanofibers Hydrogen storage textiles. Moreover, magnesium nanoparticles have extremely good

thermal absorption properties - hence they can be used in hyperthermia therapy for treating tumors[112].

Properties	Numerical Factor
Atomic number (Z)	12
Massnumber (A)	24
Gram atomic weight (g)	24.312
atomic radius (A°)	1.6
Volumetric mass (g/cm^3)	1.74
Melting point (C°)	650
boiling temperature (C°)	1107
The first ionization energy (kg/mol)	738
Electron energy (e.v)	-3.0

2.10.3Core-shell Nanoparticle

The core-shell type nanoparticles are defined as concentric core and a coating shell. Core-shell nanoparticles can be classified based on inner and outer material into organic-organic, inorganic-inorganic, organic-inorganic, inorganic-organic materials [113]. Depending on the application, shell material, as well as shape and, or structure of nanoparticles, could be chosen.

Modified properties of core-shell nanoparticles can be obtained by either changing the volume ratio of the core part to the shell part or change composite materials, such as thermal stability, reactivity, and dispersibilityofthe core [114]. The main purpose of the core part coating is to fold the surface modifications, stability and dispersibility to control the functionality of the core. Core-shell nanoparticles are widely used in many applications such as photothermal cancer therapy [115, 116],

control drug delivery [117,118], catalysis [119], optoelectronics [120], and photoluminescence [121, 122].

The optical properties of core-shell nanoparticles have high tunability dependent on the size, shape, martial composition, and the dielectric constant of an environment of core-shell nanoparticles [123,124]. Furthermore, the core-shell nanoparticle colloids of metal-dielectric show an intense surface plasmon absorption band in the visible range, which extremely sensitive to particle size and shape and electronic properties of the medium surrounding. Decreasing particle size leads to reduce the restoring force due to increasing distance between the free electrons and the ions so that the bandgap shifts to higher energies and the absorption spectrum shows a blue shift. In contrast, increase the particle size (more than 100 nm for optical frequencies) leads to higher oscillations modes and the electrons are no longer able respond homogenously to the incident field [125]. In addition to that, the surface plasmon resonance also influenced by dielectric properties (permittivity) of the surrounding media. The Incident field induces polarization of the surrounding medium around the nanoparticle surface. This medium polarization compensates some of the metal charges of nanoparticle surface and reducing the restoring force of electrons, and a redshift is occurred [126].

2.11 Surface Plasmon Resonance (SPR)

This property appears on the surfaces of some metals and it is a result of the collective movement of free electrons in the nanoparticle when a light falls on them [127]. It is a periodic movement in which the direction of electrons motion changes with a time at the same oscillation of the incident electromagnetic wave [128]. This feature is a clearly demonstrated in noble metals such as gold, silver, and copper in the

visible light region and is responsible for changing their colors when these elements reach the nano-size [129].

The researches in plasmonics have led to extensive applications in the field of optoelectronics such as light emitting diodes, waveguides, and nanoscale lasers, as a result of the surface plasmon resonance property of some metallic nanostructures [130]. In a random laser, the gain strongly depends on the strength of scattering medium where the light interacts with these disturbed amplification media in such systems [131]. The scattering is mainly occurred due to dielectric or metallic scattered nanoparticles. Metallic nanoparticles (MNPs) play an effective role in spectral narrowing more than dielectric NPs, as we mentioned in a previous section that MNPs have a much larger scattered cross section than that of the dielectric NPs at the same dimensional. MNPs, especially the noble ones, are rich in the surface plasmon resonance property, which enables the trapping of light near the surface of those particles, which in turn leads to a high gain for random laser [132]. The SPR position is strongly influenced by the material type, size, shape as well as the environment of the NPs [133]. These parameters give spectral tuning facilitates overlapping the wavelength of the SPR with the emission wavelength of the desired active medium [134]. Plasmon-enhanced metallic nanoparticles which are implanted in a randomlaser medium lead to a collective optimization in both the strength of scattering and the gain volume of the random laser. Besides, the confinement of photons near the particle's surface enhances the strength of the local field and thus increases the gain [135]. Whereas, these nanoparticles have the ability to adjust the radiative and non-radiative transition rates of nearby dye molecules [136]. In general, laser dyes have significant Stokes shifts between their absorption and emissions, which can reduce self-absorption

and achieve lower lasing threshold [137]. Emission intensity of random laser can be enhanced with the assisted of a plasmon by coupling between the dye and a localized SPR of nanoparticle [138] provided that there is a clear overlap between the surface plasmon resonance spectrum of the nanoparticles and emission spectrum of the dye.

2.12 Tunable Absorption Spectrum of Al and Mg Semi-plasmonicNanoparticles:

Al and Mg nanoparticles absorb and scatter light with extraordinary efficiency due to a strong interaction of light with conduction electrons on the metal surface of the nanoparticle. When excited by light of a specific wavelength, these conduction electrons undergo a collective oscillation known as surface plasmon resonance (SPR) and this oscillation causes the absorption and scattering intensities of Al and Mg nanoparticles to be much higher than identically sized non-plasmonic nanoparticles. Gold and silver are common examples of plasmonic nanoparticles used in nano-enabled technologies because the optical properties of these materials can be tuned throughout the visible and near-infrared (NIR) portions of the spectrum, providing a useful response for diagnostics, therapeutics, display technologies, and more. Al and Mg-based nanomaterials offer additional capabilities, with an optical response that extends into the ultraviolet (UV) region. This extension of the SPR peak into the UV region is appreciable when compared against silver and gold, as shown in the graph below [139].

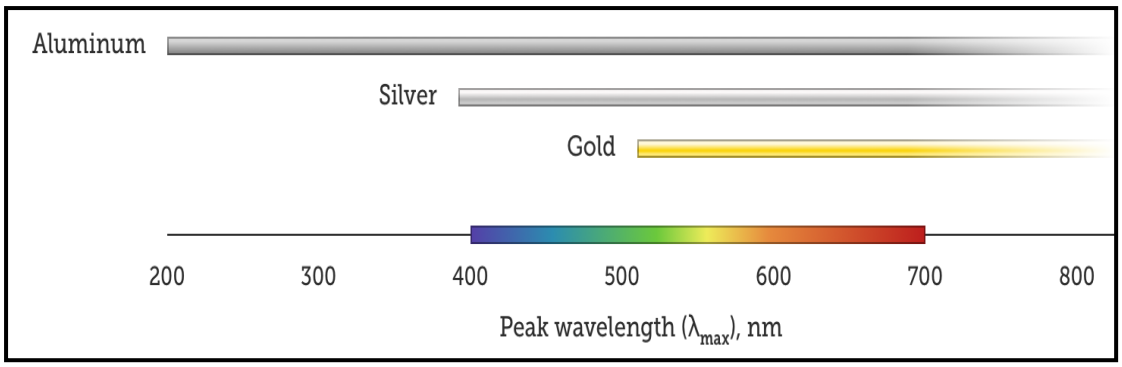

Fig. (2.6) SPR comparison of different peak nanoparticles[139]

Chapter Three

Experimental

part

3.1 Introduction

In this chapter, the properties of materials used in our experiments to generate random laser with specific outputs will be discussed. The ways and methods used in preparing the research materials will also be covered. Then, the random media will be reviewed depending on the type and concentration of the semi-plasmonic materials used as scattering centers in the random laser system. The experimental setups which employed whether to test the performance of the random laser. Also the laser ablation technique is used to produce different types of nanoparticles will be explained, and many measurement devices are employed in this work such as UV-Visible, transmission electron microscope (TEM) and random laser setup.

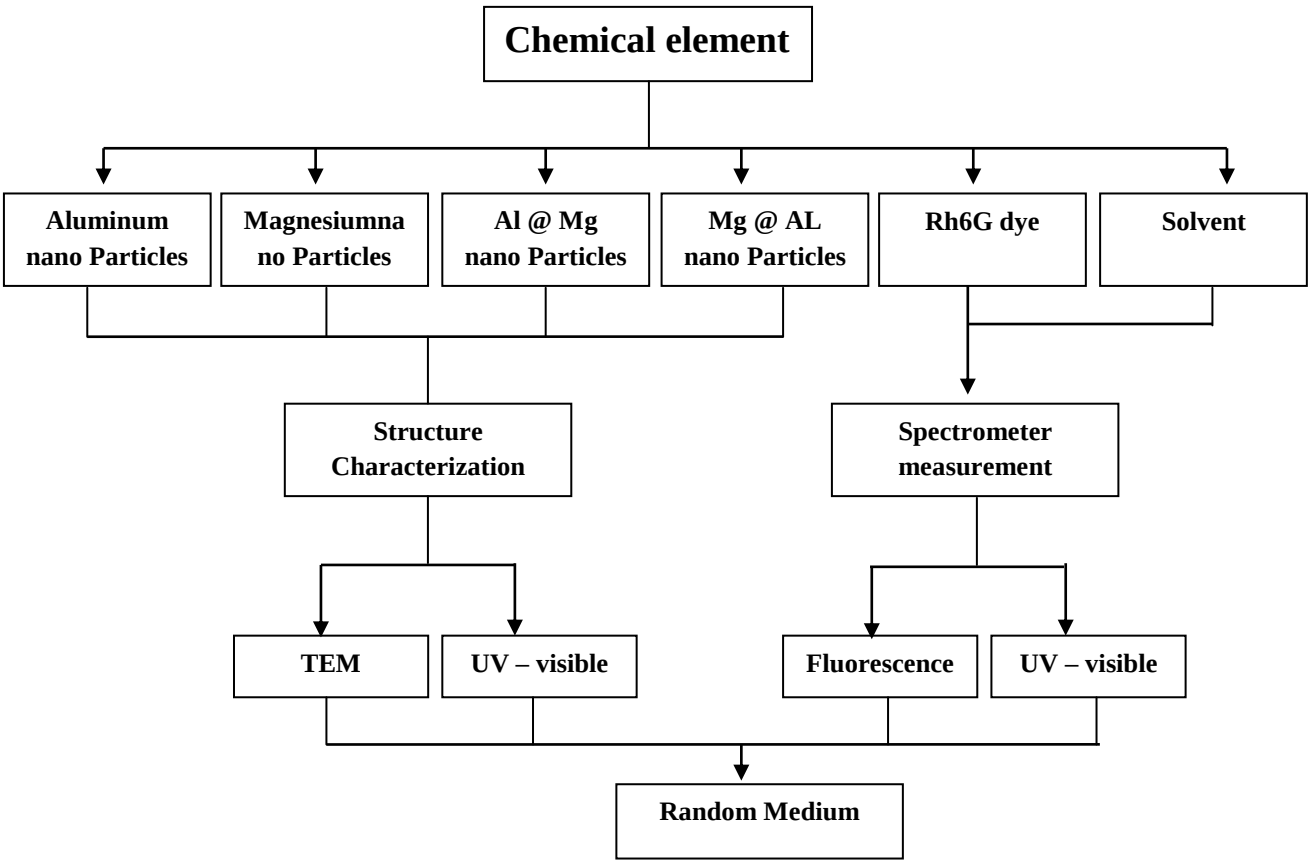

3.2 Nanoparticles Preparation

It is known that random laser output is affected by the type, shape, size, and characteristics of nanoparticles.Therefore; two groups of nanoparticles were prepared: the first group is a semi-plasmonic group (Al and Mg NPs) and the second includes semi-plasmonic core-shell group (Al@Mg and Mg@Al). These two groups will be discussed in details as follows:

3.2.1 Preparation Al and Mg Nanoparticles

Two different kinds of semiplasmonic materials such as Al and Mg NPs ware prepared by laser ablation in liquids (LAL) method, by (Al and Mg target (>99.99% purity, Sigma Aldrich, Germany) with thickness of Al target (2mm) and Mg target(3 mm), the semiplasmonic nanoparticles prepared with using Q-switched Nd: YAG laser with different pulse, the pulse width of 5 ns and repetition rate of 1–10 Hz. These samples were prepared at a fixed energy at 200 mJ and variable repetition rate. In order to get different concentrations of for each type of semiplasmonicnanoparticles, the ablation procedure was performed with five different laser pulses 500, 600, 700, 800 and 900P. It was found that increasing the laser pulse leads to the formation of a gradual increase in the concentration of the Al and Mg NPs.The laser source was focused on the target using special kind of a high reflective mirror and lens with length (25 cm) on a rotated Al and Mg metal target in a deionized water as shown in fig (3-1). The concentrations had been produced by the laser ablation were verified using a transmission electron microscopy (TEM). The optical properties of were the optical properties of nanoparticle also studied by UV-Vis spectrophotometer.

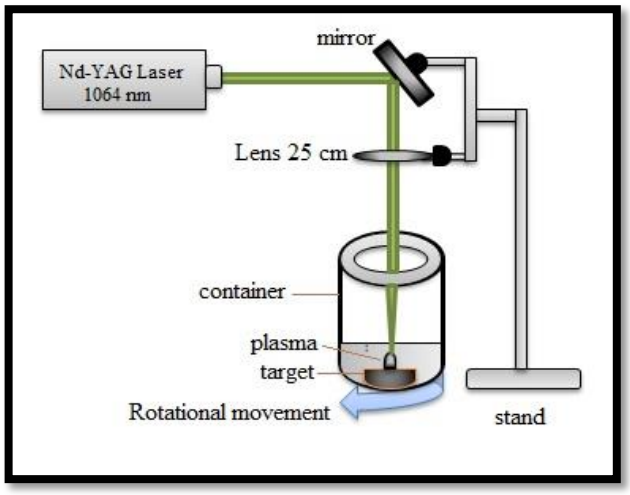

(Fig.3.1) Schematic of the experimental setup used for Al and mg nanoparticles preparation by lAL

3.2.2 Preparation Al@Mg and Mg@Al core-shell Nanoparticles

Two kinds of the core-shell NPs such as, Al@Mg and Mg@Al samples were prepared by laser Ablation in Liqwed LAL method using the first harmonic Q-switched Nd:YAG laser with fixed energy at 200 mJ, repetition rate of 10 Hz and a pulse width of 5 ns which are suitable to produce the required size of the NPs. A sequential two-steps ablation method was used: first, for Al@Mg core-shell, Al NPs colloidal solution was prepared by laser ablation at 600P and after that Mg target was put in this medium for different pulses (150 and 300P) to get the different thicknesses of Mg shell. For Mg@Al core-shell, the inverse procedure was applied; it means that at first, Mg NPs are produced in the water solution and then, changing the target to Al to get the Mg@Al NPs. The purpose of the shell thickness difference is to study the best possible result to achieve our goal.

3.3 Dye preparation

Different concentrations of dye have been produced, which were Rhodamine 6G. It was prepared with various concentrations. Rh6G were dissolved in $\mathbf{100}\boldsymbol{ml}$of methanol, the weigh selected (0.0479 g) to obtain high concentration (10^{-3} M) as according to the following formula:

$$C = \frac{W}{M_w}\frac{1000}{V}$$

Where C represents the concentration of dye solution reported in M (mol/L), W describes the weight in mg, M_w refers to the molecular weight of the dye in grams/mole (g/mol)., and V describes the volume of solvent in liter (L The high concentration of the dye which was $1*10^{-4}$ M was prepared, and the other concentrations were obtained by dilution the amount of the solvent by using the dilution law:

$$C_1V_1 = C_2V_2$$

Where C_1 and C_2 represent the available and required concentration respectively, while V_1 is the amount of solvent for the first concentration, and $V_2$is the amount of solvent assumed to be used to obtain the desired concentration. Then the process has been repeated to obtain the rest concentrations. According to the aforementioned, the following concentrations of Rh-B dye solution were obtained ($7.5*10^{-5}$ M, $5*10^{-5}$ M, $2.5*10^{-5}$ M, $1*10^{-5}$ M, $5*10^{-6}$ M, and $1*10^{-6}$M).

3.4 Mixed dye with different types of nanoparticles

After the dye have been prepared with different concentrations ($7.5*10^{-5}$ M, $5*10^{-5}$ M, $2.5*10^{-5}$ M, $1*10^{-5}$ M, $5*10^{-6}$ M, and $1*10^{-6}$M)and also semi-nanoparticles with different types, and concentrations, then we selected the best concentration from each kind of dye and mixed with different types and concentrations of nanoparticles to form various random mediums, then compare among these media to get the best results. We will try to explain that in detail.

3.4.1 Mixing of Rh6G dye with Al, Mg nanoparticles

As explained in the previous section the Rh6G dyes were separately dissolved in methanol at different concentration, after testing these concentrations under UV-Visible and emission spectrum, show us that the best concentration for each dye is (2.5x10-5 M). To obtain a gain medium in our random laser, we will mix two types of nanoparticles into this concentration of dye. To obtain a gain medium for our random laser, the best concentration of the dye will be mixed with two types of the used semi-plasmonicmaterials (five concentrations for each type), five different random media have been prepared for each type by mixing 2 ml Rh-6G with 1 ml from each concentration of Al and Mg nanoparticles to investigate the effect of nanoparticles concentration on random laser action, to compare their results of the a gain medium with the Al NPs and Mg NPs. In the second step, the fabricated samples were stirred at room temperature (RT) in an ultrasonic bath for about 20 min to obtain the best homogeneity for these samples.

3.4.2Mixing of Rh6G dye with Core-shell nanoparticles

Continuing our work to produce the best random laser, two kinds of core-shell NPs, such as Al@mg and mg@Al samples with a difference in the shell thickness, The best shell thickness was chosen with 600P and 150,300P for the core and the shell by laser ablation, respectively. Two different types and shell thickness random media have been prepared for each type by mixing 2 ml Rh-6G with 1 ml from each type of Al@Mg and Mg@Al nanoparticles. For these samples to be ready for testing, they were stirred at room temperature (RT) in an ultrasonic bath for about 20 min.

3.5Preparing random media of the different scattering centers

To characterize the performance of random lasers under the influence of a different scattering centers in terms of type, shape, size and concentration, several random media were prepared that tested by using the experimental setup shown in Fig.(3.2). this setup is consisted of a pulsed laser as pumping source with the following specifications: second harmonic generation (532 nm) of Nd:YAG pulsed laser with different pumping energies, a repetition rate of 10 Hz and a pulse duration of 5 ns. Joule meter was used to measure the pumping energy falling on the sample after it has passed through attenuator. Optical emission spectroscopy (TANSU company) to collect the random laser emission and sending to computer for analysis. Now, these various random media will be shown, briefly.

3.6 : Measuring Instruments

3.6.1 : Measurement of Absorption Spectra

The absorption spectra have several names, such as absorbance spectra, UV-Vis spectra, and electronic spectra). By this device observed the change in absorbance of a sample as a function of the wavelength of the light incident, and are measured using a UV-2601 double beam spectrophotometer covering the wavelength range from 190 to 1200 nm supplied by Ray Leigh (EnviSense, England) as shown in Figure (3.3)..

3.6.2 Transmission Electron Microscopy (TEM) Measurements

. In an effort to gain better accuracy to find out the dimensions of the core-shell nanoparticles shape, size, and the thickness. We need to use transmission electron microscopy (TEM) model (Zeiss- EM10C) operating at an accelerating voltage of 100 kV, as shown in Figure(3.3)

Fig. (3.1): Schematic of TEM device.

3.6.3 Q Switched ND YAG Laser

The Q-switched Nd:YAG laser emits a longer, near-infrared ray of 1,064 nm that is capable of penetrating into the deeper regions of the skin. Therefore, it is able to destroy deep-seated dermal melanocytes by selective photothermolysis. For this reason, many dermatology clinics commonly use this laser to treat nevus of Ota and Hori, or to remove tattoos. Its effectiveness for dermal melanocytosis treatment has been demonstrated, but problems with bleeding have prevented this laser from being used for melanocytic nevi. Based on this information, we postulated that control of bleeding can facilitate removal of melanocytic nevi with the Q-switched Nd:YAG laser, since nevi have a histology similar to the nevus of Ota and Hori. This study investigated this hypothesis

Fig (3.2) Q Switched ND YAG Laser

.

3.6.4 Fluorescence Spectrometer

The SCINCO FS-2 fluorescence spectrometer delivers exceptional sensitivity for the most accurate measurements. Take your analysisto the next level of clarity with an industry leading 0.5 nm spectral bandwidth for both emission and excitation measurements.Accessories for temperature control, solid samples, and polarization give you sampling flexibility. Build a complete system for your laboratory with our extensive line of accessories. Powerful FluoroMaster Plus software helps you move seamlessly from data acquisition to reporting results.

Chapter Four

Result and discussion

4-1 Introduction

In this chapter, the structure characterizations of the prepared samples were determined by TEM. With regard to optical characteristics, we will study the absorption spectrum for each for semeplasmonicmetal group (Al, Mg, AL@Mg, Mg@AL), And also the absorption and fluorescence spectrum of (Rh6G dye) with and without mixed with nanoparticles, it was determined to find the appropriate concentrations for our work. The result of the spectral study also includes semsplasmonic multi-wavelength random laser emission tests for different concentrations and gain media In these tests, we used fixed pump energy for reach to coherent random lasing, and also to determine the laser threshold for each sample. Then to compare between our results for each concentration, we measured scattering mean free path, FWHM, and peak intensity..

4.2Properties Of The Prepared Sample

Fig(4.1)(a-f) represents the images of the Al NPs and Mg NPs prepared by the laser ablation method in deionized water as a host medium. in the fig (4.1)(a-c) observed transmission electron microscopy (TEM) of Al NPs with low, model, and high concentrations which corresponds to (500, 700, and 900 P) with fixed energy pulses at (200 mJ), and also the images show the formation of Al NPs by grain size range(60-80) and(55-80)nm. In the same above condition, the (TEM) image of Mg NPs appears with a grain size approximately from(55-80)nm, and the sizes were determined by imageJ program.

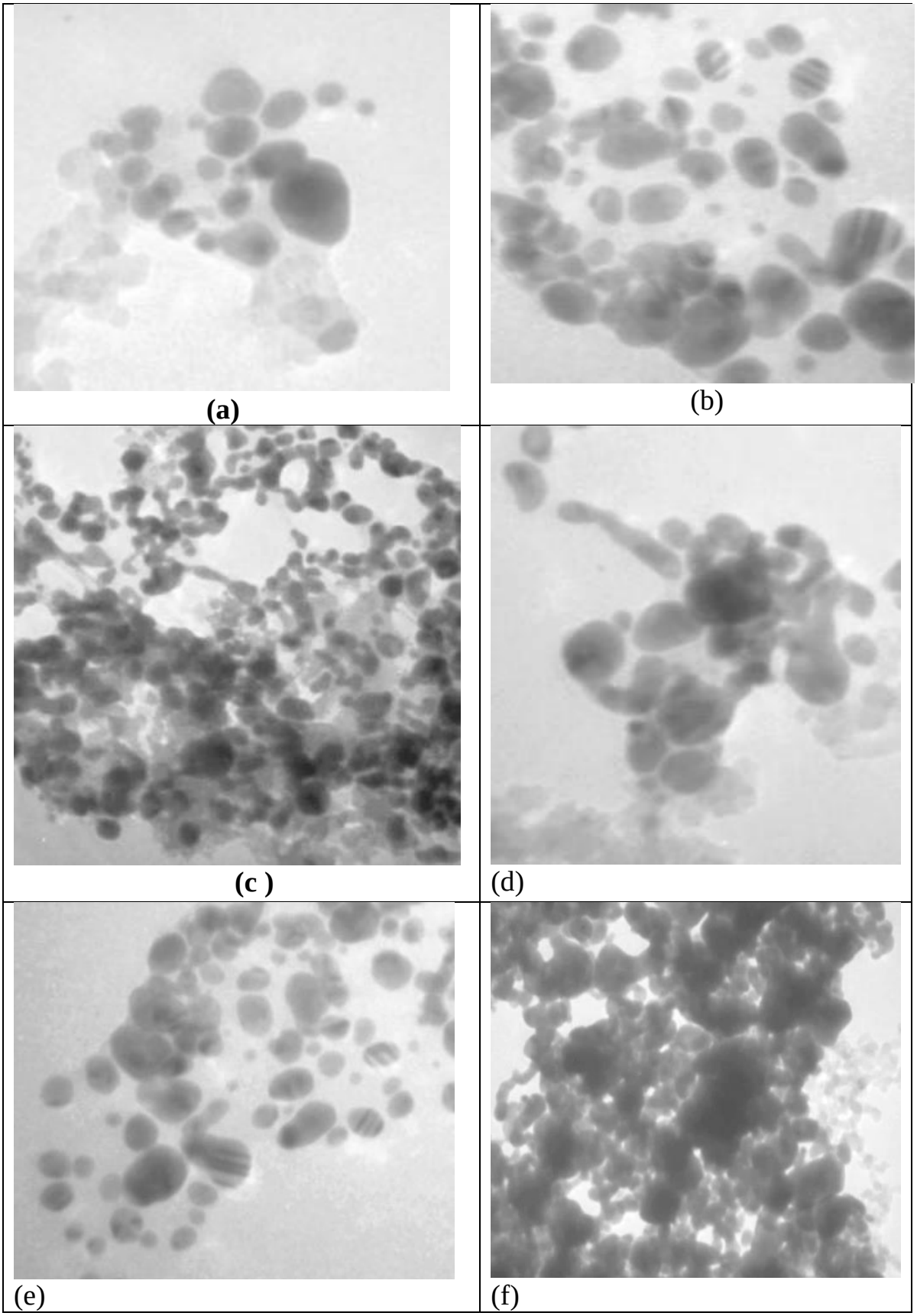

Fig(4.1) TEM images of the colloidal solutions with different concentrations: (a-c) Al NPs (500, 700, and 900 P), (d-f) Mg NPs (500, 700, and 900 P) respectively

4.2 The Optical Properties Of The Prepar Sample

Absorption spectra with different concentrations of the Al NPs and Mg NPs were measured straightway after ablation by the spectrophotometer as shown in Fig. (4.1).in the experimental part, semi Plasmonic NPs prepared at different namber of pulses and at fixed energy (200 mj) have shown SPR absorption spectrum as indicated by their NPs concentrations.The Al NPs and Mg NPs exhibited large absorption in the ultraviolet range, and the edge of the absorption band extended towards the visible region.the absorption curve of Al NPs increased by increasing the number of laser pulses of nanoparticles in the solution as shown in fig 4 a, the absorption spectrum of Al NPs of five concentrations, while observed the absorption carve with high concentrations (violet carve) more highest than low concentrations, Also, it is found that increasing the of Mg NPs concentrations gives rise to an increase in the absorption efficiency as shown in fig 4 b, and This behavior is obvious in the (black curve) is have highest absorption curve than from the lower concentrations.

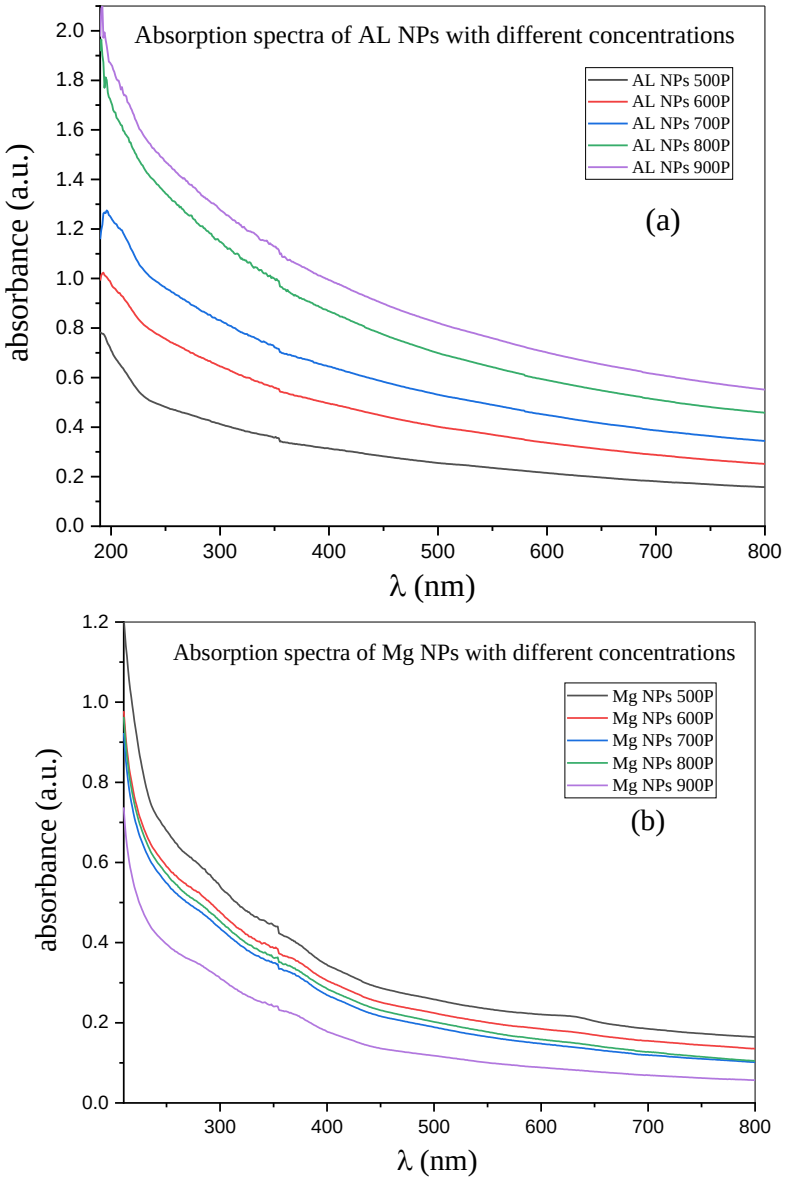

*Fig.(4.2) The absorption spectrum of (a) Al NPs (b)Mg NPs***.**

The absorption spectra of Rh6G dye with different concentrations ($1x10^{-6}$, $5x10^{-6}$, $1*10^{-5}$, $2.5x10^{-5}$, $5x10^{-5}$, and $7.5x10^{-5}$M) which dissolved in ethanol have been studied, as shown in Fig. (4.1)(c), and can be observed that with increasing the concentration of the dye in the ethanol solution, the absorption peak increase with its maximum peak at 530 nm. Therefore, the best absorption spectrum of Rh6G dye was obtained at concentrations $2.5x10^{-5}$ M at 530 nm. Thus, this concentration will be adopted for the remainder of our active random gain media after mixing with different semiplasmonic nanoparticles.

The fluorescence spectra for the different concentrations of Rh6G dye were illustrated in Fig. (4.1)(d) using (Scinco fluorescence spectrometer), the intensity of the emission spectrum, increases with increasing dye concentration to a certain extent of focus afterwards behavior is reflected, a decrease in intensity fluorescence is observed with an increase in the concentration of the dye. The best emission spectrum appears in the concentrations $2.5x10^{-5}$ M for this reason this have been choose it as a suitable concentration for the active gain media based on the absorption spectrum.

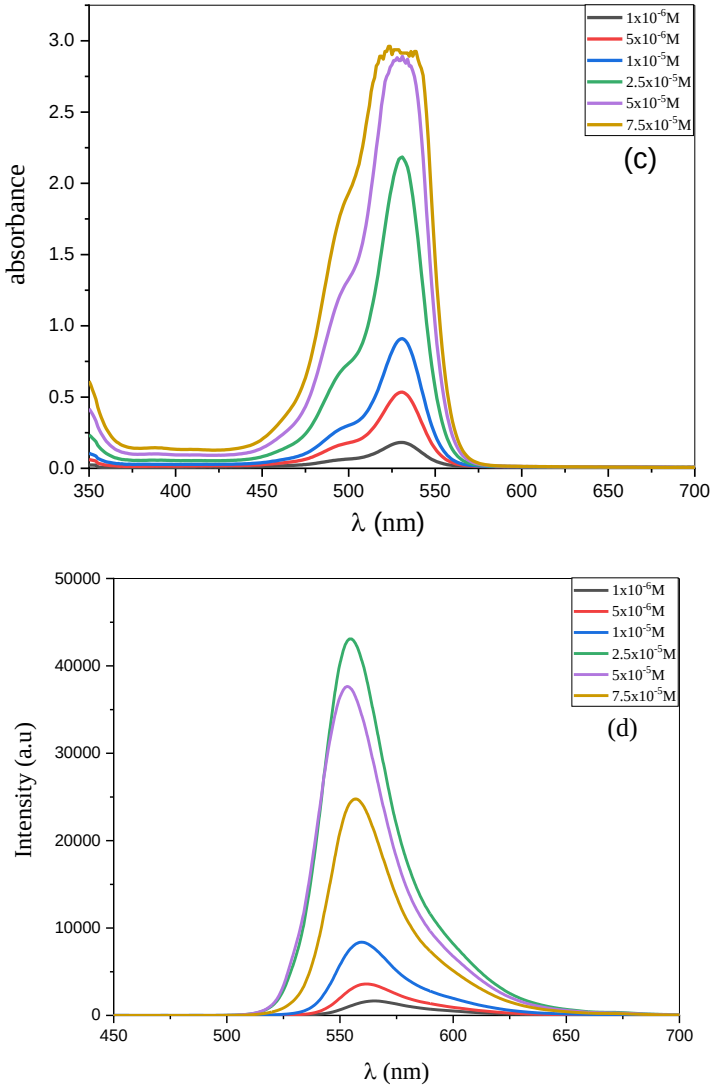

Fig. (4.3)(a) Absorption spectra of Rh6G dissolved in ethanol with different concentration, (b) Fluorescence spectrum of Rh6G at different concentrations

We also tested the fluorescence of Rh6G dye at different concentrations under green laser source (532 nm), and that also confirmed to us the best concentration is $2.5x10^{-5}$M, as shown in the real fluorescence in the figure (4.4)

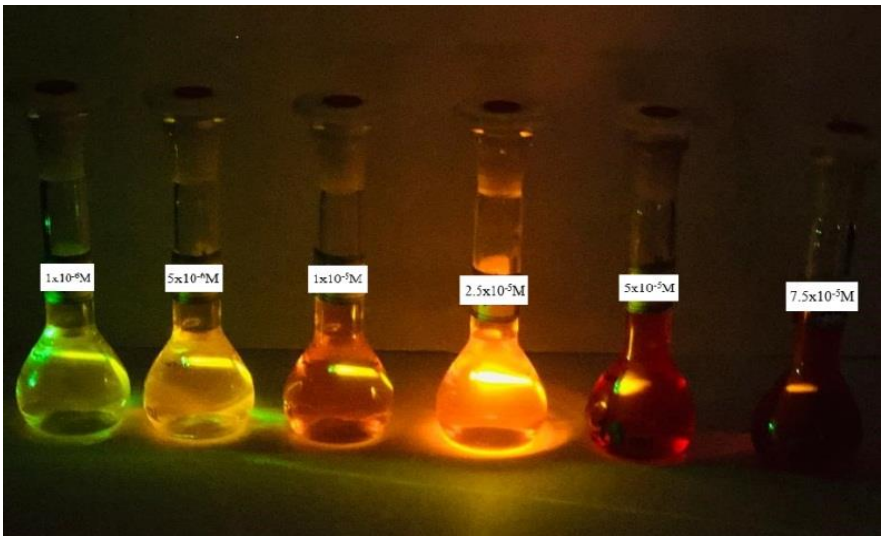

Fig.(4.4)Real image emission spectra due to different concentrations of dyes without nanoparticles.

Al NPs and Mg NPs absorb and scatter light with high efficiency due to a strong interaction of light with conduction electrons on the metal surface of the nanoparticle. When Al NPs and Mg NPs mixed with the best concentration of Rh6G dye ($2.5x10^{-5}$ M) and excited by the suitable wavelength, the same wavelength that it absorbed dye.Thus, these electrons are responsible for the collective oscillation on the surface to form the plasmonic phenomenon (SPR), and this phenomenon increases the absorption and scattering ratio inside active gain media, which leads to an increase in the emission spectrum when adding it to the active media with appropriate concentrations when the concentrations of nanoparticles are increased more than the appropriate limit, they affect to the fluorescence spectrum, causing quenching in the emission spectrum as shown in the fig (4.5).The best fluorescence spectrum in active random media appears with a concentration of Al NPs (800 P), and it has been seen in the violet carve in the fig (4.5 a), and it has a peak intensity of the

fluorescence spectrum at (35700 a.u.), also,it has been observed the best concentration using Mg NPs was in the (800P) as shown in the red curve in the fig (4.5b), In this type of nanoparticle the peak intensity of the active medium was observed at (41650 a.u.). From this, we deduce the Mg NPs has more strong scatterers than Al NPs.

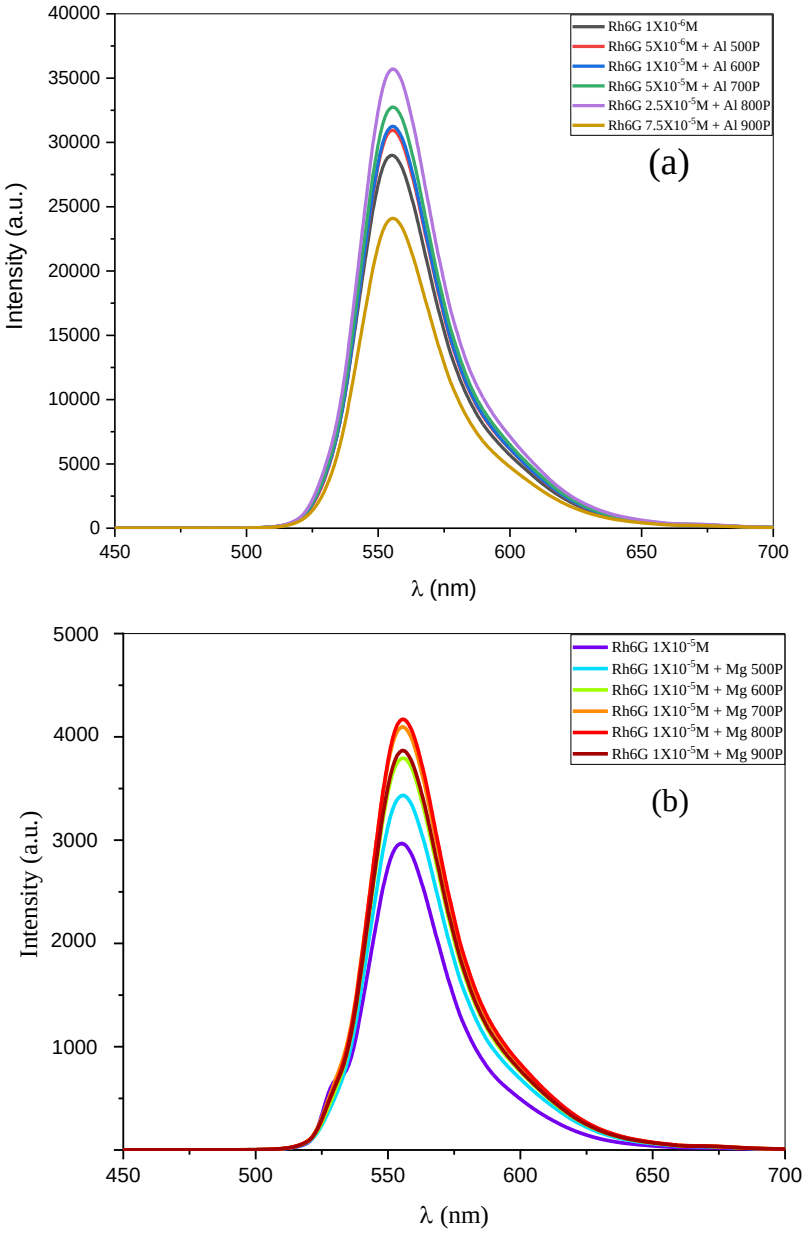

Fig. (4.5) Fluorescence spectrum of R6G mixed with different concentrations of nanoparticles, (a) Al NPs and (b) Mg NPs

4.3 Random laser by Al NPs

The emission spectra of random active gain medium mixed with five concentrations of Al NPs and which it pumped by 532 nm have been investigated. As shown in the fig (6 a) the random laser properties observed withlow concentration of Al NPs (500 P) mixed with Rh6G with (2.5x10-5 M), in this active random medium remarked the intensity enhanced gradually when the increased energy pumping from (25 to 70 μJ), At the lowest pumping energy 25 mJ, It is noticed that there is no random laser appearing in this energy, when increased energy pumping on the active media, this lead to increases in the peak of intensity, and the FWHM decreases, this behavior refers to the emergence and incoherent random laser it was observed at a threshold equal 55 μJ, after enhanced energy pumping the peak intensity increased to reach (9600 a.u.) and FWHM (14 nm) and the number of spikes also increased in the emission spectrum with the width of these peaks can reach less than 1 nanometer, which is one of the most important indicators of the transition from incoherent random lasers to coherent random lasers. So the concentration of semiplasmonic nanoparticles within active media has a basic role enhance of emission spectrum, and it also clearly affects the transition from an incoherent to a coherent random laser.

After that, the 500 P of Al NPs will be replaced by the Al with 600P which as shown in Fig. (4.6 b) represents the random laser properties when increasing the concentration of Al NPs to 600P.the emission peak begins to narrower and its intensity rises more rapidly with increasing pumping energy, the lasing threshold is reduced to (50μJ) in the new concentration, and the FWHM appears to be more narrow with the value of (13.1) with an increased number of spikes and has higher peak

intensity than the previous concentration and its value is estimated (12700 a.u).

Now a third concentration of the gain medium will be generated by adding Al NPs 700P. As Fig. (4.6 c) exhibited that the properties of this random laser compared with previous concentrations have been enhanced. Therefore, increasing the concentration of Al NPs in the random medium will improve the properties of the random laser due to increase the scattering centers in this concentration, the most important of which is the surface plasmon resonance. Where we notice a clear increase in the peak intensity reach (16500 a.u.), the lasing threshold at (45 μJ), and the value of FWHM about (12.9), also with an enhanced number of spikes at the top of the peak of the intensity.

We will continue to increase the concentration of the Al NPs 800P. It is observed from Fig. (4.6 d) that the peak intensity of the emission spectrum increase super linearly with increasing pumping energy to reach about (19000 a.u.), and the value of FWHM reaches (12.5)with more spikes in the peak of the intensity, as observed the best threshold in this concentration (40μJ). The dramatic decrease in the lasing threshold in this concentration under test is due to the increased plasmonic scattering centers in the gain medium, which has the property of a surface plasmon that enables the material to be trapped photons near the surface, creating an improved gain area near the surface of the material and thus accelerates the occurrence of the random coherent laser.This result corresponds to the fluorescence spectrum, as shown in Fig (5 a).

The high concentrations of Al NPs 900P have a direct effect on the scattering mean free path as well as on lasing threshold, as observed the peak intensity was increased in the previous case but decreased in higher

concentration. Thus, the more reduction of the scattering mean free path led to a lower lasing threshold. This leads to the confinement of the photon longer period inside the active medium due to the increase in the number of nanoparticles, and this increase does not allow the photon to transition to the dye which is considered the main source of the gain, thus leading to producing obstructs which don't allow to escaping the photons from the active medium easily. So the peak intensity in this case has value (11700 a.u.), and increase in the lasing threshold value reach to at (45 μJ) again, and the value of FWHM about (13 nm), this behavior can be seen in the fig (4.6 e).

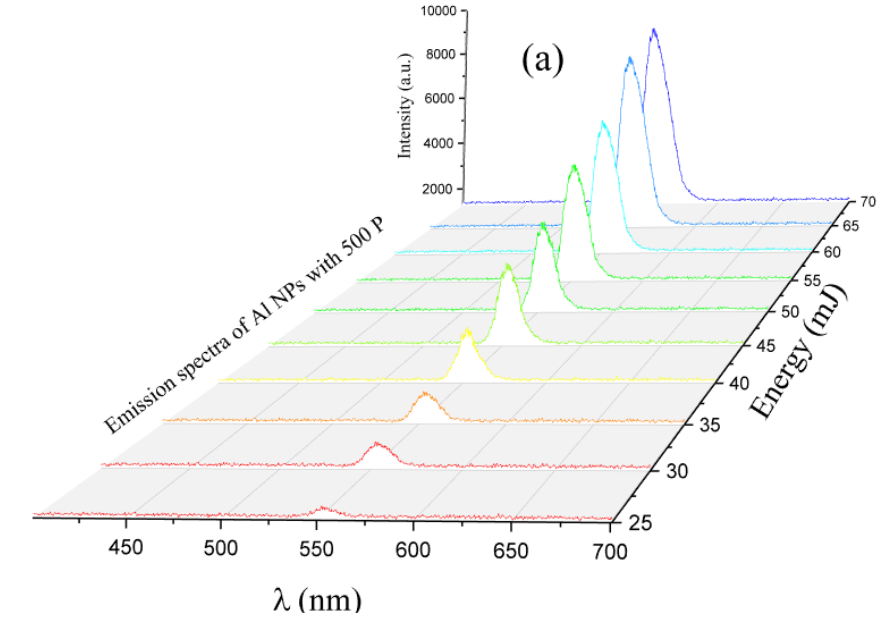
(a)
Intensity (a.u.)
10000
8000
6000
4000
2000
Emission spectra of Al NPs with 500 P
Energy (mJ)
70
65
60
55
50
45
40
35
30
25
450
500
550
600
650
700
λ (nm)

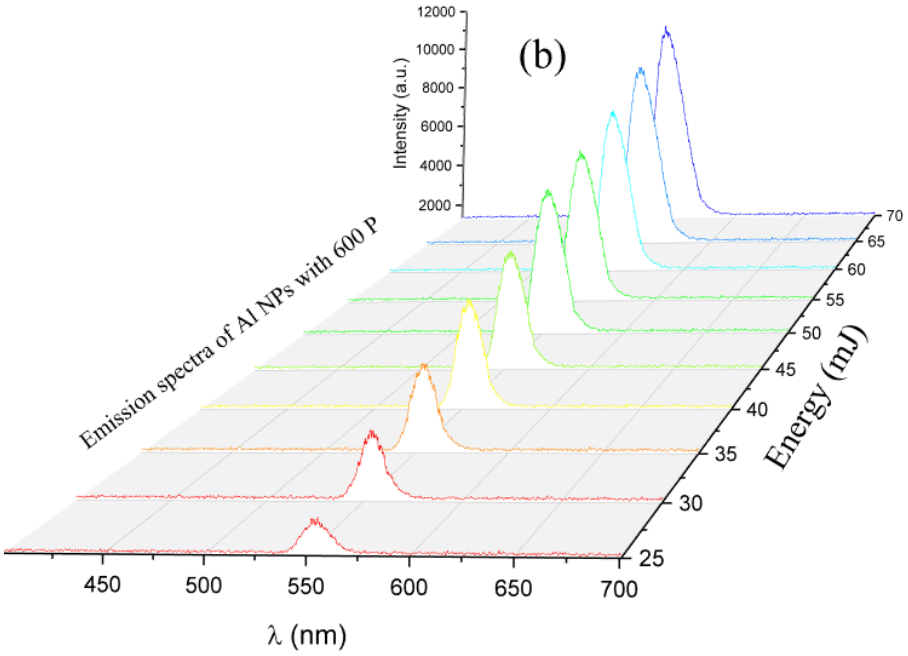
(b)
Intensity (a.u.)
12000
10000
8000
6000
4000
2000
Emission spectra of Al NPs with 600 P
Energy (mJ)
70
65
60
55
50
45
40
35
30
25
450
500
550
600
650
700
λ (nm)

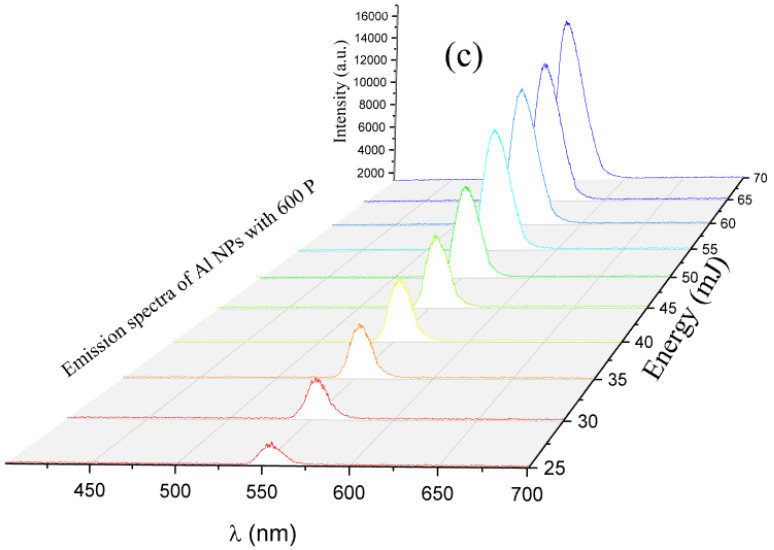
(c)
Intensity (a.u.)
16000
14000
12000
10000
8000
6000
4000
2000
Emission spectra of Al NPs with 600 P
Energy (mJ)
70
65
60
55
50
45
40
35
30
25
450
500
550
600
650
700
λ (nm)

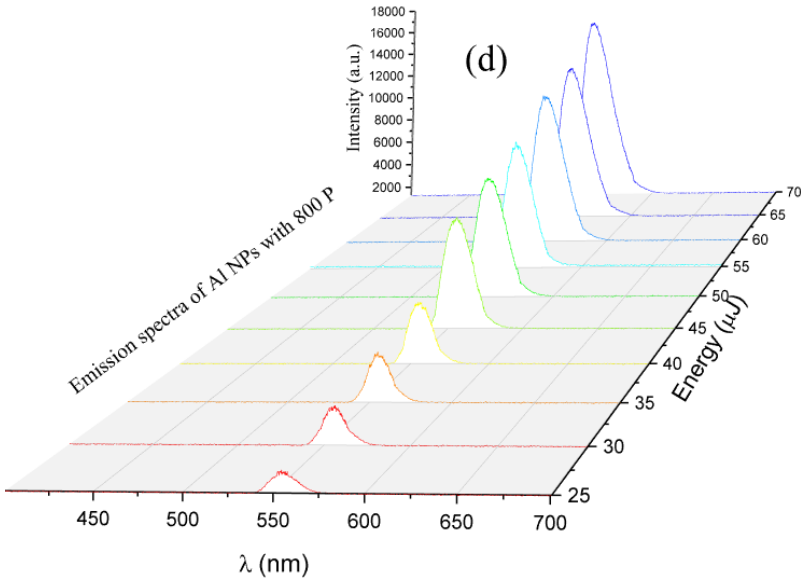
(d)
Intensity (a.u.)
18000
16000
14000
12000
10000
8000
6000
4000
2000
Emission spectra of Al NPs with 800 P
Energy (μJ)
70
65
60
55
50
45
40
35
30
25
450
500
550
600
650
700
λ (nm)

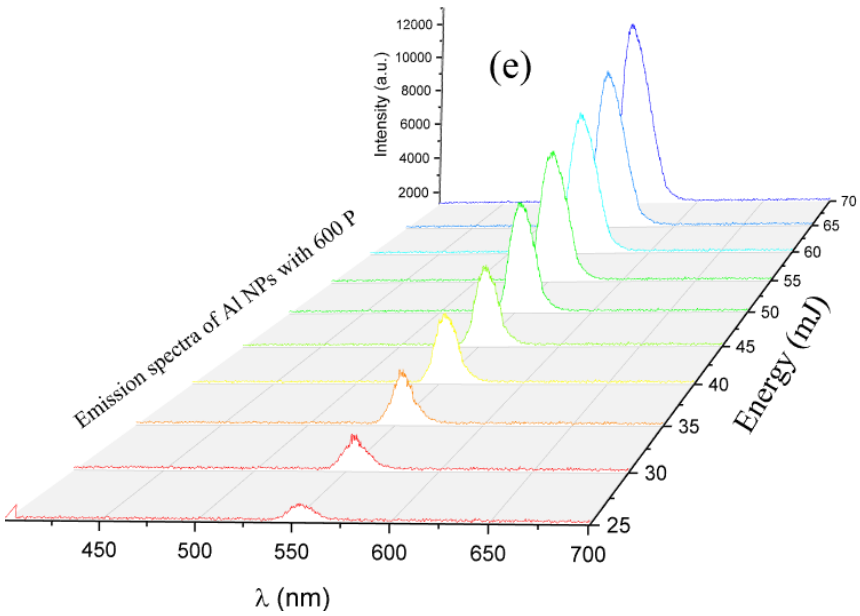
(e)
Intensity (a.u.)
12000
10000
8000
6000
4000
2000
Emission spectra of Al NPs with 600 P
Energy (mJ)
70
65
60
55
50
45
40
35
30
25
450
500
550
600
650
700
λ (nm)

Fig.(4.6) The emission intensity of the Rh6G with five samples of Al NPs concentrations 500P, 600P, 700P, 800P, and 900P as function of the pumping energy.

Fig.(4.7 a) allows a comparison between the lasing threshold for five different concentrations of Al NPs. The sample with Al NPs 800P shows a low pumping threshold of about 40 μJ, while the remainder of random laser systems has lasing thresholds is 55, 50, 45, and 40μJ according to the ratio of the Al NPs concentrations in random media 500P, 600P, 700P, and 500P respectively. Where Fig.(7 b) shows that the (FWHM) narrows as the proportion of Al NPs concentrations increases except for the concentration of Al NPs 900P in the gain media. Moreover, when the pumping energy increases the width of the (FWHM) narrows until it reaches to settles.

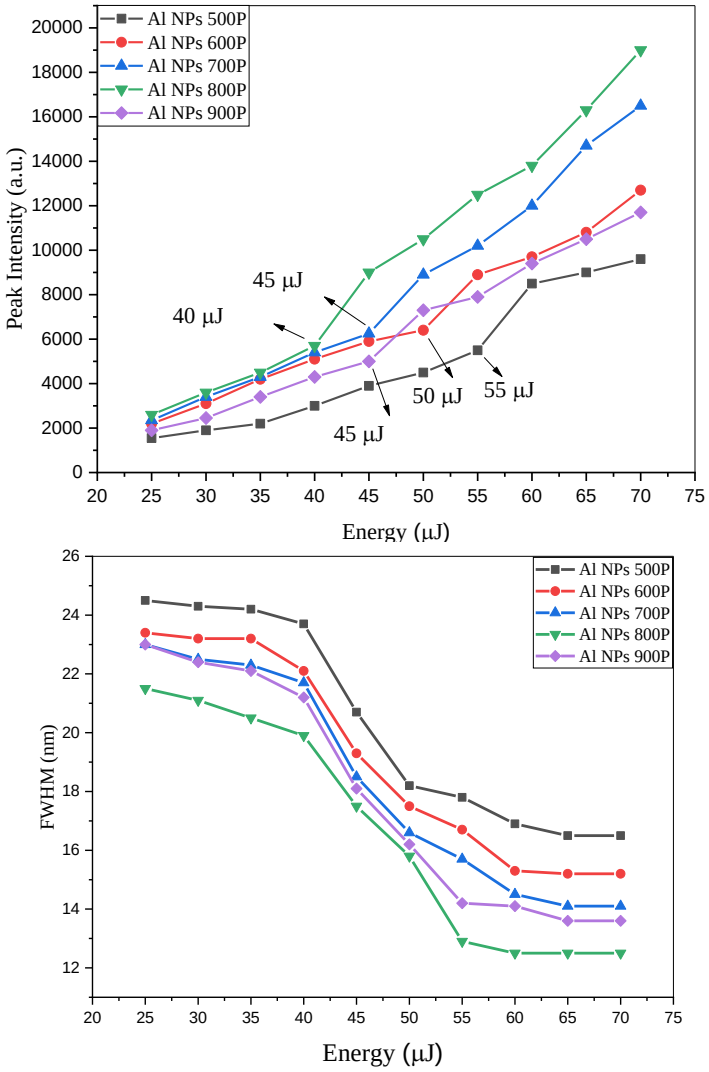

Fig.(4.7) (a) the peak intensity as function of pumping energy. (b) FWHM as function of pumping energy.

In the fig (4.8), the effect of the concentration of Al NPs on the emergence of these spikes in addition to their number will be discussed. as it was observed that their emergence was related to the lasing threshold for the emitted spectrum of a random laser, when increased pumping energy is above the threshold, the gain is more than the loss in random cavities, and the photons in this case oscillate to add separate peaks to the emission spectrum, and the number of spikes with an increase in the widthagaininthe emission spectrum reduces by increasing the

concentrations of Al NPs to 900P despite the increase in the number of scattering centers.

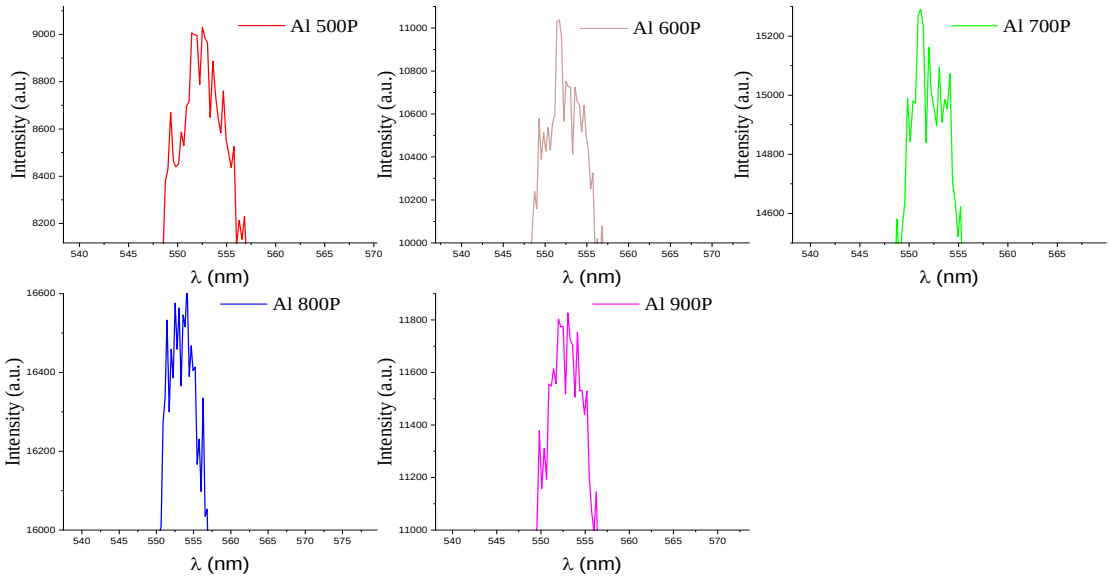

Fig.(4.8) the evolution of the spikes with different Al NPs concentrations

For analysis, the parameters of mean free path can be calculate by the formula(1.7) for each concentrations with the cell thickness of T, the transmitted intensity of the solvent (I_0) and the transmitted intensity of the solvent with Al NPs (I) should be investigated.

then, it is observed that the mean free path for Al NPs with 800P concentration is smaller than that of lower concentrations NPs for this reason, It was obtained more gain in the emission spectra based on the suitable concentration of Al NPs with 800P was added to the dye, and this concentration has a direct effect on the scattering mean free path as well as on lasing threshold and peak intensity, In other words, we get the greatest gain in the active media when the value of the mean free path decreases. The peak intensity was low in the low and high concentration 900P. Thus, the increase in the scattering mean free path led to the high lasing threshold as shown in the table (1).

Sample	Peak intensity (a.u.)	FWHM (nm)	Threshold (μJ)	l_s (mm)
Al 500P	9600	16.5	55	0.79
Al 600P	12700	15.2	50	0.72
Al 700P	16500	14.4	45	0.66
Al 800P	19000	12.5	40	0.59
Al 900P	11700	13.6	45	0.68

Table (1) represents some of the random laser parameter

4.4 Random laser by Mg NPs

As mentioned above, the scattering centers of these types of nanoparticles have high efficiency due to a strong interaction of light with conduction electrons on the surface of the nanoparticle. To investigate the effect change in the Mg NPs concentration on random laser action, the emission spectra of five samples were measured as explained in the experimental setup in fig (2). Where it's recorded at different pumping energy, the measured results represented in Fig.(4.9 a-e) are shown that the emission spectrum begins to increase gradually with increasing the Mg NPs concentration. The demeanor of the properties of random laser in relation to the first four concentrations of Mg NPs is a common behavior where the intensity increases and both the lasing threshold and FWHM decrease with increasing the concentration. But what is noticed, was a sudden change occurred when the Mg NPs concentration continued to increase to 900P, as the emission intensity decreased while the lasing threshold and FWHM increased and this can be attributed to the quenching of

luminescence which occurs when the location of the metallic NPs become a very close to the dye molecules.

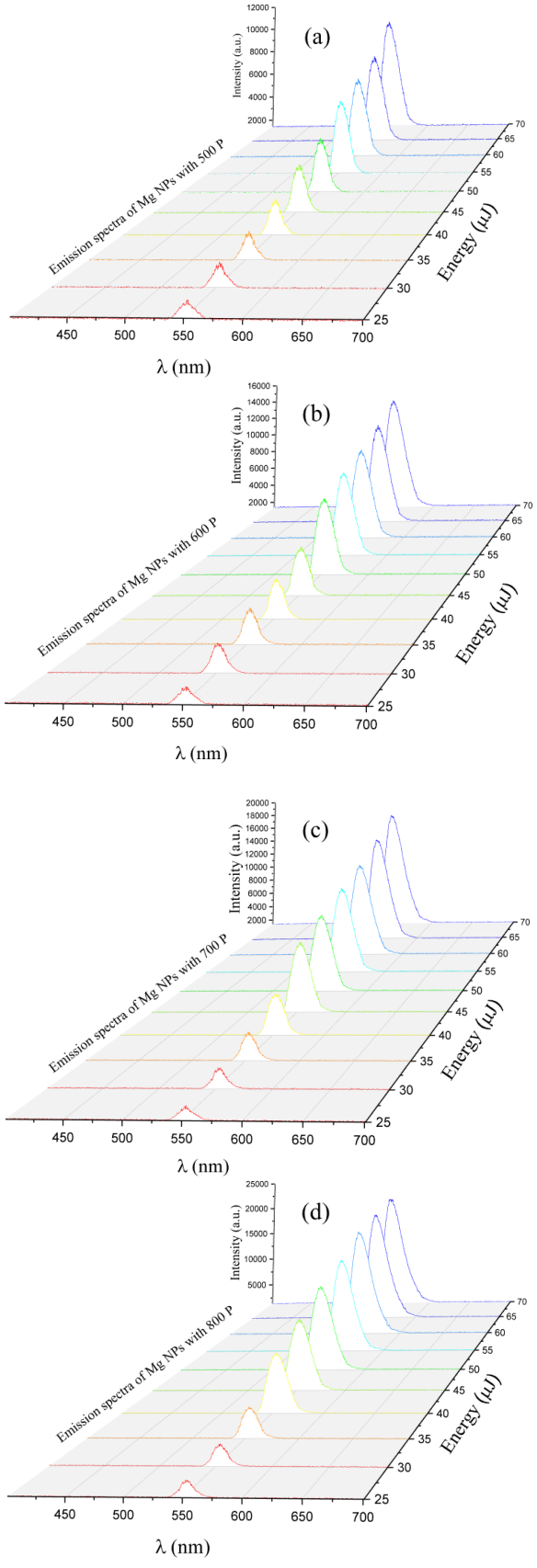

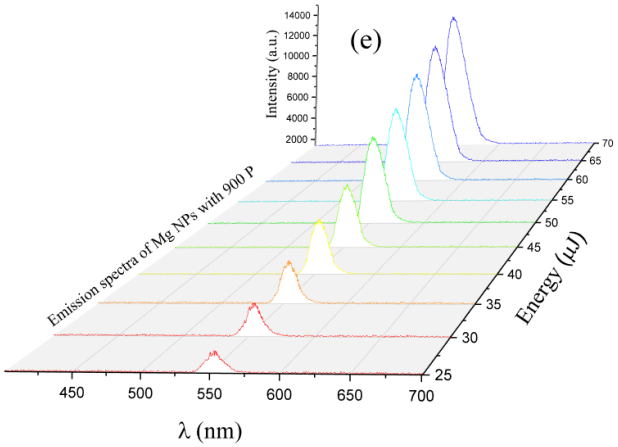

Fig.(4.9) The emission intensity of the five samples of MgNPs with concentrations 500P, 600P, 700P, 800P, and 900P as function of the pumping energy

So, the intensity of the emission gradually increases from 10500, 13800, 17500, until it reaches to 215400 a.u. when the concentration of Ag NPs increases from 500, 600, 700 to 800P. But this increase in the emission intensity does not continue and a sudden drop occurs in it, so that it decreases to 13500 with Mg NPs 900P.The same goes for the lasing threshold, as it was found that increasing the Mg NPs concentration leads to decrease in the lasing threshold from 50 to 35 μJ when the particle concentration increases from 500P to 800P. But at certain degree of concentration, the lasing threshold begins to increase rapidly to reach 45μJ with increasing the concentration to 900P as shown in Fig. (4.10 a).As for the FWHM, Fig.(4.10 b) shows that the value of FWHM decreases from 14.8 to 10.5 nm when increasing Mg NPs concentration from 500 to 800P. After that, the FWHM value increases to reach 12.6 nm with increasing the concentration of the scattering particles to 900P.

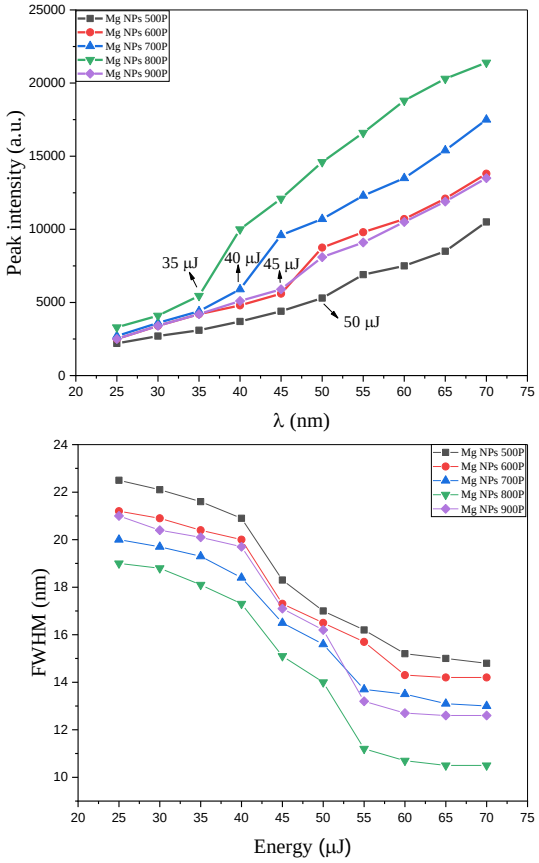

Fig.(4.10) (a) the peak intensity as function of pumping energy. (b) FWHM as function of pumping energy.

The appearance of these spikes under the influence concentration of the semiplasmonic nanoparticles, they have been covered in some detail in the Al NPs, as it was observed that their emergence was related to the threshold of the random laser. As shown in fig (4.11) it has been found that these spikes grow clearly and their number increases with increasing the Mg NPs from 500 to 800P within the dye.

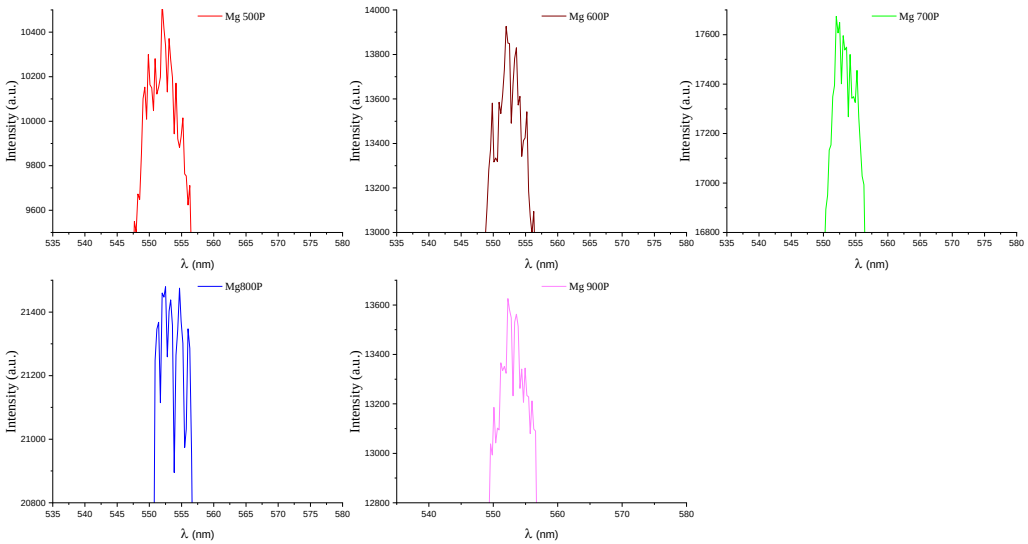

Fig.(4.11) the evolution of the spikes with different Al NPs concentrations

From table (2) the value of the l_s and FWHM will be reduced by increasing Mg NPs concentration since they are inversely proportional to their concentration, thus the higher the concentration, the lower their values.

Table (2) represents some of the random laser parameters

Sample	Peak intensity (a.u.)	FWHM (nm)	Threshold (μJ)	l_s (mm)
Mg 500P	10500	14.8	50	0.71
Mg 600P	13800	14.2	45	0.63
Mg 700P	17500	13	40	0.58
Mg 800P	21400	10.5	35	0.53
Mg 900P	13500	12.6	40	0.65

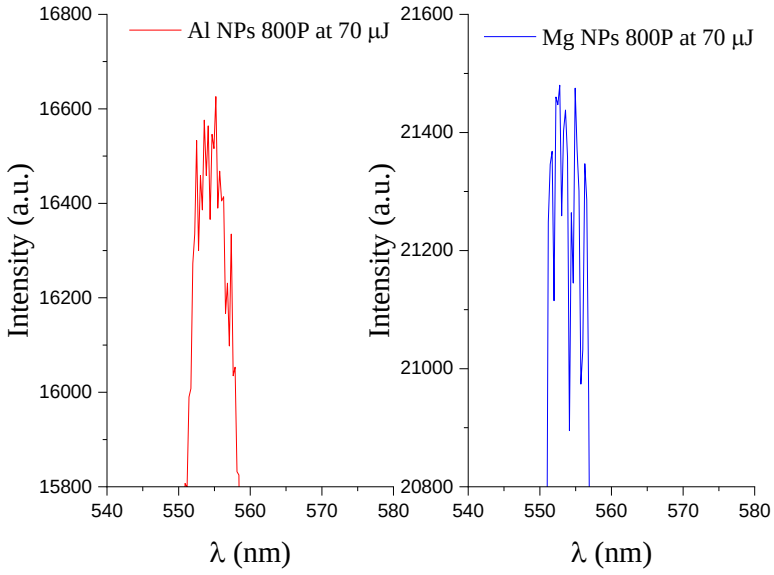

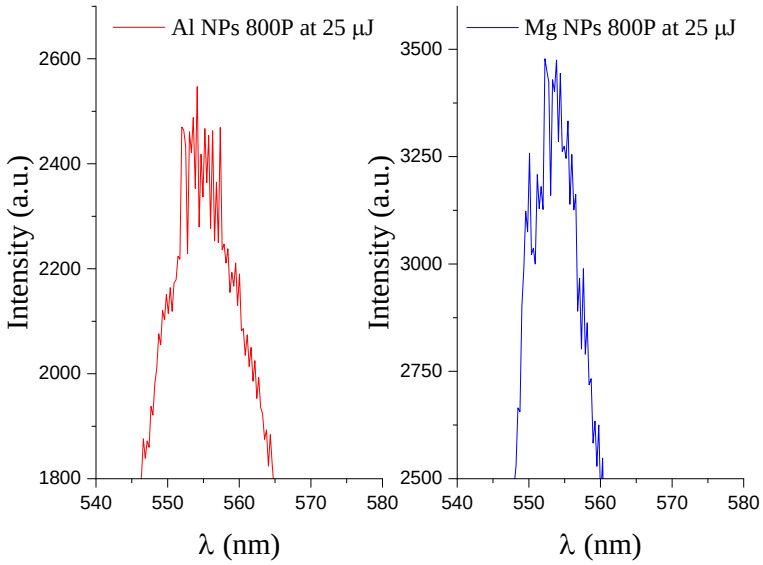

Fig.(4-12) the peak intensity and spikes with the effect of the type of the scattering centers for the low and high pumping energy**.**

4.5 Random laser by core- shell NPs

In this part, a new type of gain medium was studied which contains different concentrations and shell thicknesses of metallic core-shell (Al@Mg, Mg@Al NPs) mixed with a fixed concentration of Rh6G ($2.5x10^{-5}$M) with a high quantum yield (~1) as a gain medium. To achieve coherent lasing, the effect of NP interface of the core-shell style is important for changing the absorption and mainly their scattering. In addition, we have an efficient overlap, adjustable and tunable SPR wavelength by changing the shell thickness, effective volume of the main core and the host medium of the NPs. As shown in Figure. 4-13 (a and b) , there are two main peaks for the core-shell NPs with 500P and(100 and 200P) for the core and shell ablation respectively; which comes from different shell thicknesses of as it measured by TEM images in Fig.4-14.

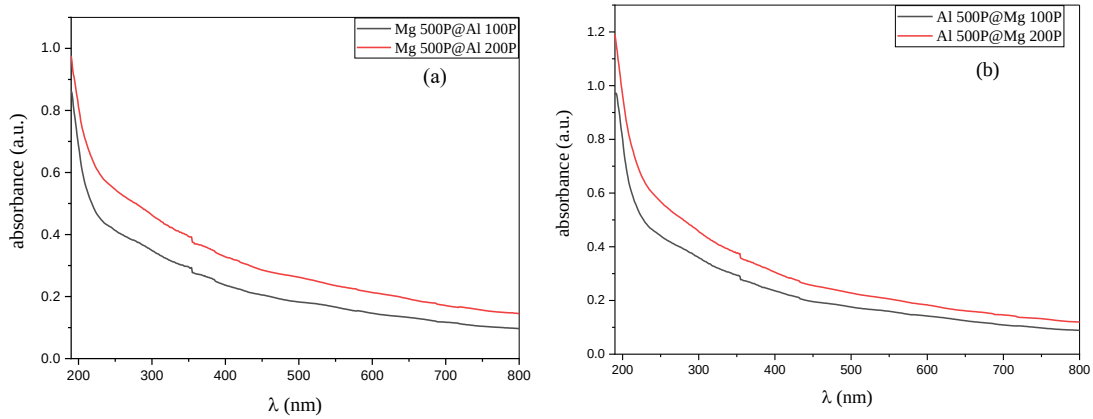

Fig.(4.13) The absorption spectrum of (a) Mg@Al*(b)*Al@Mg *NPs.*

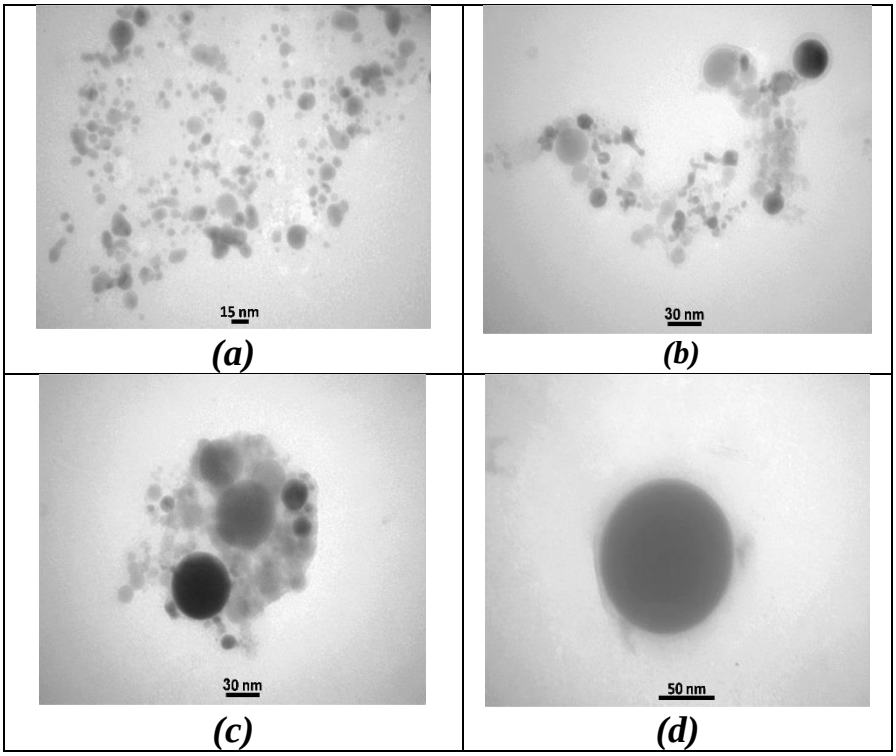

Fig.(4.14) *TEM image of* ***(a)*** *Mg@Al****(b)****Al@Mg* ***NPs.***

Rh6G dye was chosen as a gain medium dispersed in methanol where the effect of the local field enhancement on lasing resonance in Al@Mg and Mg@Al core-shell NPs was investigated. There are many factors that can reduce the threshold gain such as the ratio of the shell thickness to the core radius. The threshold gain could be remarkably reduced when the ratio of the shell thickness to the core radius is increased to some extent. This will reduce the amount of light energy lost in core as well.

Therefore, it was naturally anticipated that the lowest threshold would occur at a certain shell thickness as shown in the fig. 4.15.

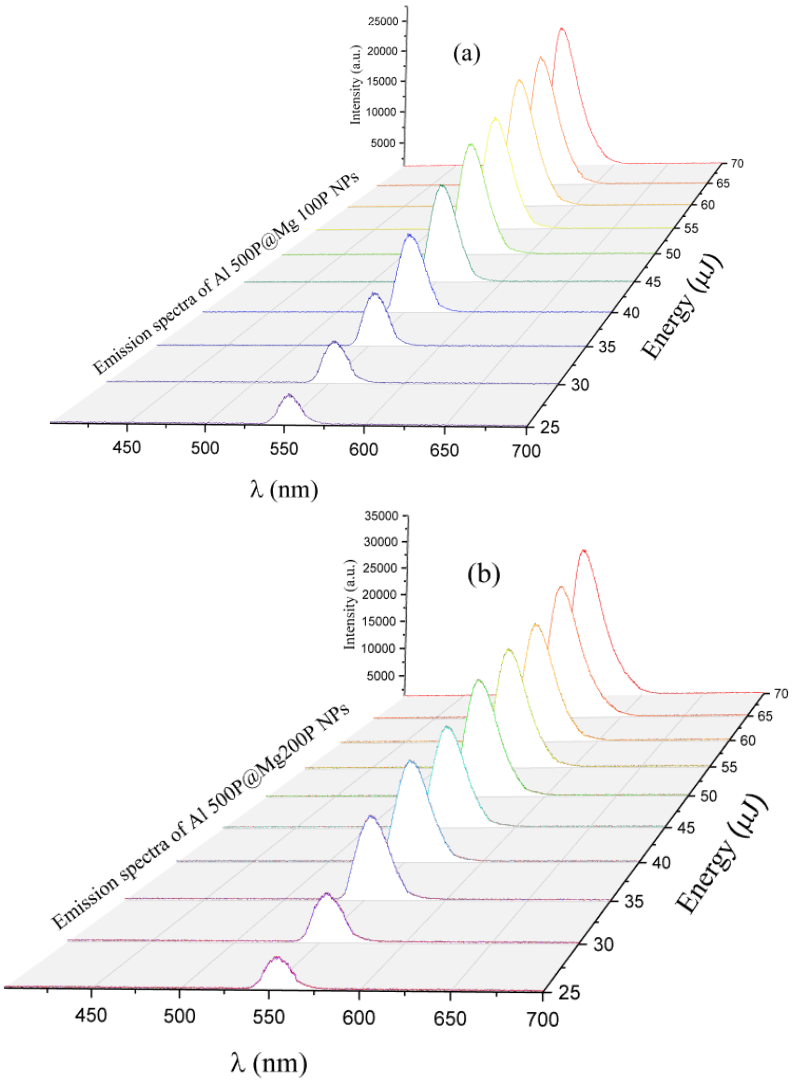

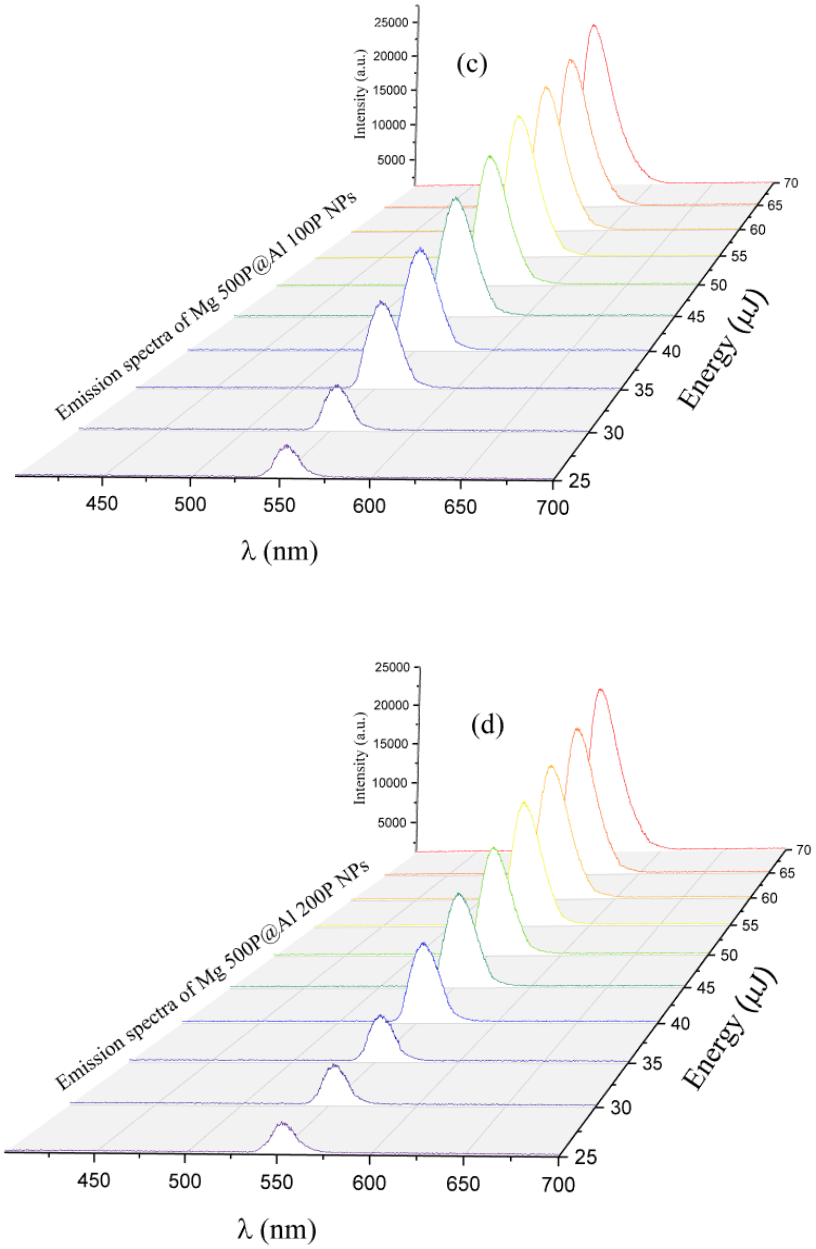

Fig.4-15: The emission spectrum of different shell thickness of Al@Mg and Mg@Al in Rh6G.

The threshold characteristics of Al@Mg and Mg@Al NPs were studied as shown in figure. (4.15). It is obvious that the threshold gain of Mg@Al 100P NPs is lower than that of Al@Mg 100Pbecause of its much larger scattering cross section. The lowest pump threshold occurred near the edge of the diffusive regime corresponding to a scattering mean free path

in the first case with Al thin shell mixed with Rh6G where the transmission is decreased. Thus, the scattering mean free path reduced in Mg@Al100P resulting in the lower lasing threshold. However, the transmitted intensity increased in thin Al shell and the scattering mean free path enhanced which produced a greater lasing threshold. For Al@Mg200P and Mg@Al 200P, lasing peak is observed at 558.8 nm with FWHM of 8.7nm and 9.8nm and lasing threshold of30 and 35μJ, respectively as shown in the fig.(4.16).

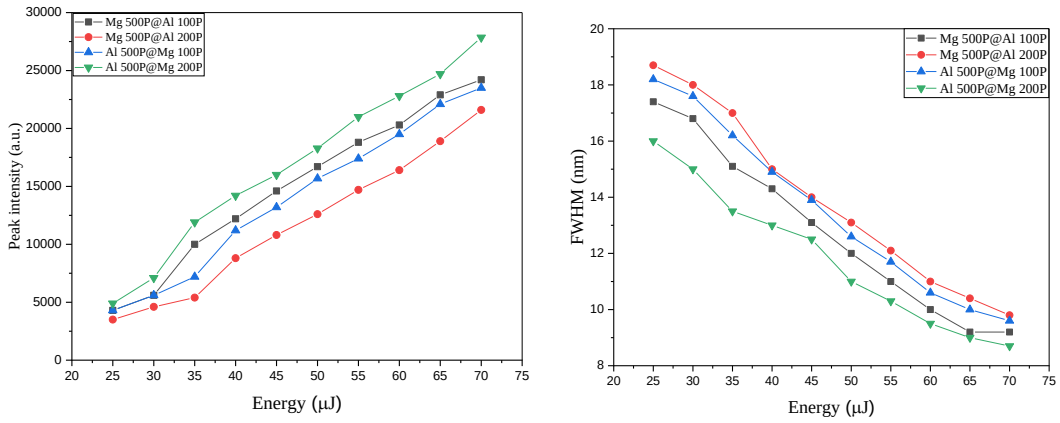

Fig.(4.16) (a) the peak intensity as function of pumping energy. (b) FWHM as function of pumping energy.

Table (3): The parameters characteristics of different concentrations of Al@Mg and Mg@Al

Sample	Peak intensity (a.u.)	FWHM (nm)	Threshold (μJ)	l_s (mm)
Mg@Al 100P	24200	9.2	30	0.42
Al @ Mg 100P	23500	9.6	35	0.45
Mg@Al 200P	21600	9.8	35	0.48
Al @ Mg 200P	27850	8.7	30	0.38

NPs

As shown in fig (4.17) it has been found that these spikes grow clearly and their number increases with increasing the Mg NPs shell from 100 to 200P within the dye.

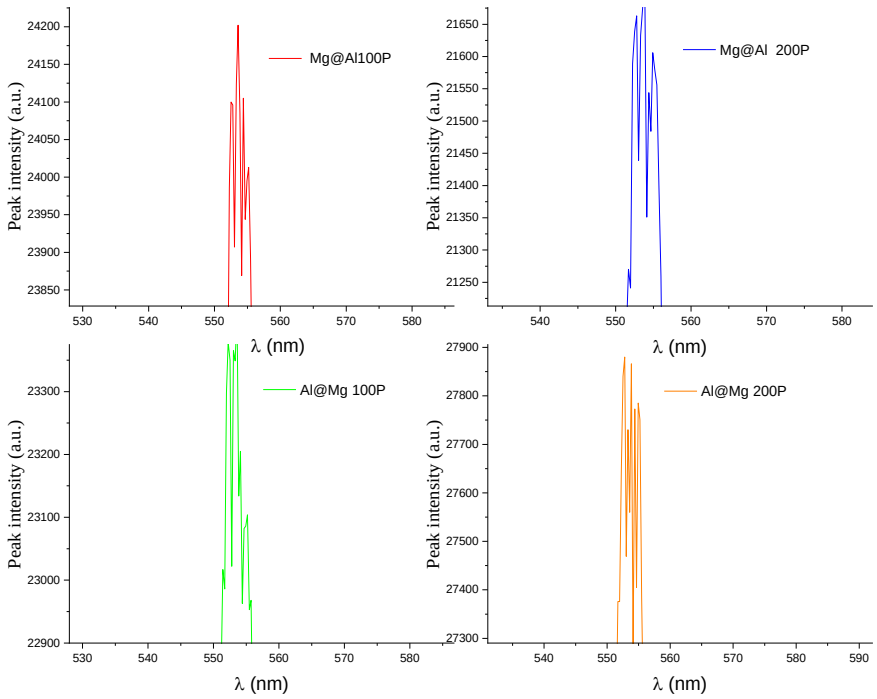

Fig.(4.17) the evolution of the spikes with Al@Mg and Mg@Al NPs with different shell thickness.

4.6 Conclusion

1-The characteristics of the random laser can improve with increased semiplasmonic nanoparticles, but the increase in the semiplasmonic nanoparticles concentration within the dye is not free, but it is limited within a certain range because the excessive concentration of the nanoparticles may lead to the quenching of fluorescence, which in turn causes a shorter lifetime and lower the quantum yield.

2- The type of semiplasmonic nanoparticles selected as scattering centers in the random medium has a great effect on the properties of the random laser,.

3- It is noticed the random laser with Mg NPs that shows better results than the Al NPs through the apparent increase in the intensity of the emission at the same pumping energy. Also, the pumping threshold of this type has materialized early compared to Al NPs, in addition, the appearance of spikes in this sample preceded the previous one.

4- In the core-shell NPs, the lasing threshold in Al@MgNPs at higher shell thickness was lower than that in the Mg@Al NPs.

4.7 Future Work

1- Using other laser dyes to study the effects on the fluorescence in the random laser and the linear optical properties, and also different types of nanoparticles as a powder can be used to study the changing in the random laser emissions.

2- To reduce lasing threshold using different shape of nanoparticles such as (nanostar, nanorise, nanorod, and nanowire nanoparticles) of different shapes and study them effect in laser operation.

References

References

[1] B. Kumar, S. K. S. Patel, N. S. Gajbhiye, and R. K. Thareja, ―Random laser action with nanostructures in a dye solution,‖ *J. Laser Appl.*, vol. 25, no. 4, p. 042012, 2013, doi: 10.2351/1.4809615.

[2] T. Okamoto and S. Adachi, ―Effect of particle size and shape on nonresonant random laser action of dye-doped polymer random media,‖ *Opt. Rev.*, vol. 17, no. 3, pp. 300–304, 2010, doi: 10.1007/s10043-010-0053-0.

[3] R. G. S. El-Dardiry and A. Lagendijk, ―Tuning random lasers by engineered absorption,‖ *Appl. Phys. Lett.*, vol. 98, no. 16, pp. 1–4, 2011, doi: 10.1063/1.3571452.

[4] D. Van Hoang, N. Thi Phuong, and N. Van Phu, ―Random Lasers: Characteristics, Applications and Some Research Results,‖ *Computational Methods in Science and Technology*, vol. Special Is, no. 02. pp. 47–51, 2010, doi: 10.12921/cmst.2010.si.02.47-51.

[5] C. S. Wang, Y. L. Chen, H. Y. Lin, Y. T. Chen, and Y. F. Chen, Enhancement of random lasing through fluorescence resonance energy transfer and light scattering mediated by nanoparticles,‖ *Appl. Phys. Lett.*, vol. 97, no. 19, pp. 1–4, 2010, doi: 10.1063/1.3515913.

[6] Yuan Wan, Yashuai An, Luogen Deng, Plasmonic enhanced low-threshold randomlasing from dye-doped nematic liquid crystals with TiN nanoparticles in capillary tubes, Sci. Rep. 7 (1) (2017),

[7] H. Zhang, G. Feng, H. Zhang, C. Yang, J. Yin, S. Zhou, Random laser based on Rhodamine 6G (Rh6G) doped poly(methyl methacrylate) (PMMA) films coating on ZnOnanorods synthesized by hydrothermal oxidation, Results Phys. 7 (2017) 2968–2972,

[8] Haddawi, Saddam F., Hammad R. Humud, Sakineh A. Monfared, and S. M. Hamidi. "Two-dimensional plasmonic multilayer as an efficient

tool for low power random lasing applications." *Waves in Random and Complex Media*, 2021, 1-10. doi:10.1080/17455030.2021.1943563.

[9] Frolov, S.V., Gellermann, W., Ozaki, M., Yoshino, K., Vardeny, Z.V.: Cooperative emission in π-conjugated polymer thin films. Phys. Rev. Lett. 78(4), 729–732 (1997). https ://doi.org/10.1103/ PhysRevLet t.78.729.

[10] Haddawi, S.F., Hammad R. Humud, and S.M. Hamidi. "Signature of plasmonic nanoparticles in multi-wavelength low power random lasing." *Optics & Laser Technology* 121 (2020), 105770. doi:10.1016/j.optlastec.2019.105770.

[11] A. Yadav, L. Zhong, J. Sun, L. Jiang, G. J. Cheng, and L. Chi, ―Tunable random lasing behavior in plasmonic nanostructures,‖ *Nano Converg.*, vol. 4, no. 1, pp. 1–8, 2017, doi: 10.1186/s40580-016-0095-5.

[12] Z. Wang *et al.*, Two-threshold silver nanowire-based random laser with different dye concentrations, *Laser Phys. Lett.*, vol. 11, no. 9, 2014, doi: 10.1088/1612-2011/11/9/095002.

[13] S. Ning*et al.*, Enhancement of amplified spontaneous emission in organic gain media by the metallic film,‖ *Org. Electron.*, vol. 15, no. 9, pp. 2052–2058, 2014, doi: 10.1016/j.orgel.2014.05.022.

[14] E. Heydari, R. Flehr, and J. Stumpe, ―Influence of spacer layer on enhancement of nanoplasmon-assisted random lasing,‖ *Appl. Phys. Lett.*, vol. 102, no. 13, 2013, doi: 10.1063/1.4800776.

[15] Murai, Shunsuke, Koji Fujita, XiangengMeng, and Katsuhisa Tanaka. "Random Dispersion of Metal Nanoparticles Can Form a Laser Cavity." Chemistry Letters 39, no. 6 (2010), 532-537. doi:10.1246/cl.2010.532.

[16] XiangengMeng, Koji Fujita, ShunsukeMurai, TomohikoMatoba, and Katsuhisa Tanaka. “Plasmonically Controlled Lasing Resonance with

Metallic-Dielectric Core-Shell Nanoparticles” Nano Letters, no 11 (2011), 374–1378, doi: 10.1021/nl200030h.

[17] Lin, Ming C., Mong-Kai Wu, Miin-Jang Chen, Jer-Ren Yang, and Makoto Shiojiri. "Blue-shifted stimulated emission from ZnO films deposited on SiO2 by atomic layer deposition." Materials Chemistry and Physics 135, no. 1 (2012), 88-93. doi:10.1016/j.matchemphys.2012.04.027.

[18] Qiao, Qian, Chong-Xin Shan, JianZheng, Hai Zhu, Siu-Fung Yu, Bing-Hui Li, Yan Jia, and De-Zhen Shen. "Surface plasmon enhanced electrically pumped random lasers." Nanoscale 5, no. 2 (2013), 513-517. doi:10.1039/c2nr32900j.

[19] Ismail, Wan Z., Deming Liu, Sandhya Clement, David W. Coutts, Ewa M. Goldys, and Judith M. Dawes. "Spectral and coherence signatures of threshold in random lasers." Journal of Optics 16, no. 10 (2014), 105008. doi:10.1088/2040-8978/16/10/105008.

[20] Ziegler, Johannes, Martin Djiango, Cynthia Vidal, CalinHrelescu, and Thomas A. Klar. "Gold nanostars for random lasing enhancement." Optics Express 23, no. 12 (2015), 15152. doi:10.1364/oe.23.015152.

[21] Zhai, Tianrui, Xiaofeng Wu, Meng Wang, Fei Tong, Songtao Li, Yanbin Ma, Jinxiang Deng, and Xinping Zhang. "Dual-wavelength polymer laser based on an active/inactive/active sandwich-like structure." Applied Physics Letters 109, no. 10 (2016), 101906. doi:10.1063/1.4962552.

[22] Jiménez-Villar, Ernesto, Iran F. Da Silva, ValdeciMestre, Niklaus U. Wetter, Cefe Lopez, Paulo C. De Oliveira, Wagner M. Faustino, and Gilberto F. De Sá. "Random Lasing at Localization T ransition in a Colloidal Suspension (TiO2@Silica)." ACS Omega 2, no. 6 (2017), 2415-2421. doi:10.1021/acsomega.7b00086.

[23] Lü, Hao, YanyanLan, Qiuling Zhao, Xia Wang, Shuaiyi Zhang, LihuaTeng, and Wing Y. Tam. "Plasmonic enhancement of random lasing from dye-doped polymer with dispersed Au nanoparticles." Applied Physics B 124, no. 12 (2018). doi:10.1007/s00340-018-7097-4.

[24] Zhang, Shuai, Junhua Tong, Chao Chen, Fengzhao Cao, Chengbin Liang, Yanrong Song, TianruiZhai, and Xinping Zhang. "Controlling the Performance of Polymer Lasers via the Cavity Coupling." Polymers 11, no. 5 (2019), 764. doi:10.3390/polym11050764.

[25] Choi, Dongsun, and Kwang S. Jeong. "Midwavelength Infrared Photoluminescence and Lasing of Tellurium Elemental Solid and Microcrystals." The Journal of Physical Chemistry Letters 10, no. 15 (2019), 4303-4309. doi:10.1021/acs.jpclett.9b01523.

[26] J. Yin, G. Feng, S. Zhou, H. Zhang, S. Wang, and H. Zhang, ―The effect of the size of Au nanorods on random laser action in a disordered media of ethylene glycol doped with Rh6G dye,‖ *Nanophotonics VI*, vol. 9884, p. 988426, 2016, doi: 10.1117/12.2225583.

[27] Z. Ren, N. Zheng, K. Ge, G. Zhang, and S. Li, ―Investigation of the LSPR on a wavelength-tunable random laser,‖ *PhysicaScripta*, vol. 94, no. 10. 2019, doi: 10.1088/1402-4896/ab07df.

[28] V. S. Gummaluri, R. Gayathri, C. Vijayan, and V. M. Murukeshan, ―Gold nano-urchins for plasmonic enhancement of random lasing in a dye-doped polymer,‖ *J. Opt. (United Kingdom)*, vol. 22, no. 6, 2020, doi: 10.1088/2040-8986/ab896b.

[29] Boardman, A.D., and A.V. Zayats. "Nonlinear Plasmonics." Modern Plasmonics, 2014, 329-347. doi:10.1016/b978-0-444-59526-3.00011-2.

[30] Lee, Byoungho, Il-Min Lee, Seyoon Kim, Dong-Ho Oh, and LambertusHesselink. "Review on subwavelength confinement of light with plasmonics." Journal of Modern Optics 57, no. 16 (2010), 1479-1497. doi:10.1080/09500340.2010.506985.

[31] Li, Ming, Scott K. Cushing, and Nianqiang Wu. "Plasmon-enhanced optical sensors: a review." The Analyst 140, no. 2 (2015), 386-406. doi:10.1039/c4an01079e.

[32] Unser, Sarah, Ian Bruzas, Jie He, and Laura Sagle. "Localized Surface Plasmon Resonance Biosensing: Current Challenges and Approaches." Sensors 15, no. 7 (2015), 15684-15716. doi:10.3390/s150715684.

[33] Caucheteur, Christophe, Tuan Guo, and Jacques Albert. "Review of plasmonic fiber optic biochemical sensors: improving the limit of detection." Analytical and Bioanalytical Chemistry 407, no. 14 (2015), 3883-3897. doi:10.1007/s00216-014-8411-6.

[34] Jain, Prashant K., Xiaohua Huang, Ivan H. El-Sayed, and Mostafa A. El-Sayed. "Review of Some Interesting Surface Plasmon Resonance-enhanced Properties of Noble Metal Nanoparticles and Their Applications to Biosystems." Plasmonics 2, no. 3 (2007), 107-118. doi:10.1007/s11468-007-9031-1.

[35] Mayer, Kathryn M., and Jason H. Hafner. "Localized Surface Plasmon Resonance Sensors." Chemical Reviews 111, no. 6 (2011), 3828-3857. doi:10.1021/cr100313v.

[36] Pelton, Matthew, and Garnett W. Bryant. Introduction to metal-nanoparticle plasmonics. Vol. 5. John Wiley & Sons, 2013.

[37] S. a Maier, Fundamentals and Applications Plasmonics : Fundamentals and Applications, Vol. 677, 2004.

[38] O'Neil, Michael P. "Synchronously pumped visible laser dye with twice the efficiency of Rhodamine 6G." Optics Letters 18, no. 1 (1993), 37. doi:10.1364/ol.18.000037.

[39] Kurian, Achamma, Nibu A. George, Binoy Paul, V. P. Nampoori, and C. P. Vallabhan. "Studies on Fluorescence Efficiency and Photodegradation of Rhodamine 6G Doped PMMA Using a Dual Beam Thermal Lens Technique." Laser Chemistry 20, no. 2-4 (2002), 99-110. doi:10.1080/02786270215153.

[40] Sathy, P., Reji Philip, V. P. Nampoori, and C. P. Vallabhan. "Fluorescence quantum yield of rhodamine 6G using pulsed photoacoustic technique." Pramana 34, no. 6 (1990), 585-590. doi:10.1007/bf02846435.

[41] Beija, Mariana, Carlos A. Afonso, and José M. Martinho. "Synthesis and applications of Rhodamine derivatives as fluorescent probes." Chemical Society Reviews 38, no. 8 (2009), 2410. doi:10.1039/b901612k.

[42] "Figure 2: Surface-enhanced Raman scattering (SERS) spectra of rhodamine-6G (R6G)." (n.d.). doi:10.7717/peerj.4361/fig-2.

[43] Scavennec, Andre, and Norris S. Nahman. "Active and passive mode locking of continuously operating rhodamine 6G dye lasers." 1974. doi:10.6028/nbs.ir.73-347.

[44] Ruby, Stanley L. "Induced Currents in Multiple Resonant Scattering." 1998. doi:10.2172/9931.

[45] [45] "LIGHT OPTICS, ELECTRON OPTICS AND WAVE MECHANICS." Principles of Optics, 1980, 738-746. doi:10.1016/b978-0-08-026482-0.50023-2.

[46] "Absorption and Scattering by an Arbitrary Particle." Absorption and Scattering of Light by Small Particles, 2007, 57-81. doi:10.1002/9783527618156.ch3.

[47] "Lasers with Nonresonant Feedback and Laserlike Emission from Powders: Early Ideas and Experiments." Solid-State Random Lasers (n.d.), 1-9. doi:10.1007/0-387-25105-7_1.

[48] "Multiple scattering of laser light from turbid water." Joint Conference on Sensing of Environmental Pollutants, 1971. doi:10.2514/6.1971-1098.

[49] "Scattering in Random Media, General scattering in random media scattering in random media." Formulas of Acoustics, 2008, 238-241. doi:10.1007/978-3-540-76833-3_77.

[50] "Scattering of Pulse Waves from a Random Distribution of Particles." Wave Propagation and Scattering in Random Media, 2010. doi:10.1109/9780470547045.ch5.

[51] A. Ishimara "Wave Propagation and Scattering in Random Media." 1978. doi:10.1016/b978-0-12-374701-3.x5001-7.

[52] Wiersma, Diederik S., Paolo Bartolini, Ad Lagendijk, and Roberto Righini. "Localization of light in a disordered medium." Nature 390, no. 6661 (1997), 671-673. doi:10.1038/37757.

[53] Tishkovets, V.P. "Multiple scattering of light by a layer of discrete random medium: backscattering." Journal of Quantitative Spectroscopy and Radiative Transfer 72, no. 2 (2002), 123-137. doi:10.1016/s0022-4073(01)00059-0.

[54] Olga, Korotkova. "Weak scattering of random beams." Random Light Beams, 2017, 319-353. doi:10.1201/b15471-8.

[55] Van der Mark, Martin B., Meint P. Van Albada, and Ad Lagendijk. "Light scattering in strongly scattering media: Multiple scattering and weak localization." Physical Review B 37, no. 7 (1988), 3575-3592. doi:10.1103/physrevb.37.3575.

[56] Hitchen, Christopher J. "The Effect of Suspension Medium Refractive index on the particle size analysis of quartz by laser diffraction." Particle & Particle Systems Characterization 9, no. 1-4 (1992), 171-175. doi:10.1002/ppsc.19920090123.

[57] Balachandran, R. M., N. M. Lawandy, and J. A. Moon. "Theory of laser action in scattering gain media." Optics Letters 22, no. 5 (1997), 319. doi:10.1364/ol.22.000319.

[58] Ivanov, V. V. "The mean free path of a photon in a scattering medium." Astrophysics 6, no. 4 (1973), 355-367. doi:10.1007/bf01001630.

[59] Yin, Jiajia, GuoyingFeng, Shouhuan Zhou, Hong Zhang, Shutong Wang, and Hua Zhang. "The shape effect of Au particles on random laser action in disordered media of Rh6G dye doped with PMMA polymer." Journal of Modern Optics 63, no. 19 (2016), 1998-2002. doi:10.1080/09500340.2016.1184338.

[60] Frank-Kamenetskii, D. A. "The Mean Free Path and the Collision Cross Section." Plasma, 1972, 139-140. doi:10.1007/978-1-349-01552-8_46.

[61] Chen, Shujing, Jinwei Shi, Xiangyu Kong, Zhaona Wang, and Dahe Liu. "Cavity coupling in a random laser formed by ZnO nanoparticles with gain materials." Laser Physics Letters 10, no. 5 (2013), 055006. doi:10.1088/1612-2011/10/5/055006.

[62] Tse, Aaron C. "Laser action and weak photon localization in random scattering media with gain." (n.d.). doi:10.14711/thesis-b484322.

[63] Cao, H., Y. G. Zhao, S. T. Ho, E. W. Seelig, Q. H. Wang, and R. P. Chang. "Random Laser Action in Semiconductor Powder." Physical Review Letters 82, no. 11 (1999), 2278-2281. doi:10.1103/physrevlett.82.2278.

[64] Ilan, Boaz, and Arnold D. Kim. "Radiative Transfer of Light in Strongly Scattering Media." Springer Series in Light Scattering, 2019, 63-103. doi:10.1007/978-3-030-03445-0_2.

[65] Lisyansky, A. A., J. H. Li, and A. Z. Genack. "Measuring the transport mean free path using a reference random medium." Optics Letters 20, no. 1 (1995), 4. doi:10.1364/ol.20.000004.

[66] Bahoura, Messaoud, and M. A. Noginov. "Determination of the transport mean free path in a solid-state random laser." Journal of the Optical Society of America B 20, no. 11 (2003), 2389. doi:10.1364/josab.20.002389.

[67] Illarramendi, M. A., M. Al-Saleh, I. Aramburu, R. Balda, and J. Fernández. "Transport mean-free-path in K5Bi1-xNdx(MoO4)4 laser crystal powders." Photonic Metamaterials: From Random to Periodic, 2006. doi:10.1364/meta.2006.thd9.

[68] Bouvy, Claire, EvgenyChelnokov, Wladimir Marine, Robert Sporken, and Bao-Lian Su. "Quantum Size Effect and very localized random laser in ZnO@mesoporous silica nanocomposite following a two-photon absorption process." Journal of Non-Crystalline Solids 355, no. 18-21 (2009), 1152-1156. doi:10.1016/j.jnoncrysol.2009.01.053.

[69] Burin, A. L., M. A. Ratner, H. Cao, and R. P. Chang. "Model for a Random Laser." Physical Review Letters 87, no. 21 (2001). doi:10.1103/physrevlett.87.215503

[70] Yi, Jiayu, GuoyingFeng, Liling Yang, Ke Yao, Chao Yang, Yingsong Song, and Shouhuan Zhou. "Behaviors of the Rh6G random laser comprising solvents and scatterers with different refractive indices." Optics Communications 285, no. 24 (2012), 5276-5282. doi:10.1016/j.optcom.2012.06.094.

[71] Cao, Hui. "Random Lasers with Coherent Feedback." Topics in Applied Physics (n.d.), 303-330. doi:10.1007/3-540-44948-5_14.

[72] Popov, O., A. Zilbershtein, and D. Davidov. "Random lasing from dye-gold nanoparticles in polymer films: Enhanced gain at the

surface-plasmon-resonance wavelength." Applied Physics Letters 89, no. 19 (2006), 191116. doi:10.1063/1.2364857.

[73] Sakuma, Ken, Naoto Hirosaki, and Rong-Jun Xie. "Red-shift of emission wavelength caused by reabsorption mechanism of europium activated Ca--SiAlON ceramic phosphors." Journal of Luminescence 126, no. 2 (2007), 843-852. doi:10.1016/j.jlumin.2006.12.006.

[74] Ghisler, CH., W. Lüthy, and H.P. Weber. "Reabsorption in a neodymium fibre laser." Optics & Laser Technology 25, no. 1 (1993), 25-29. doi:10.1016/0030-3992(93)90152-6.

[75] Brunner, W., and R. W. John. "Doppler-shift decoupling of radiation reabsorption in expanding laser-produced plasmas." Laser and Particle Beams 9, no. 4 (1991), 817-828. doi:10.1017/s0263034600006571.

[76] Acquista, Charles. "Wave propagation through a random medium: The random slab problem." Radio Science 13, no. 6 (1978), 963-968. doi:10.1029/rs013i006p00963.

[77] Premaratne, Malin, and Govind P. Agrawal. "Light propagation through dispersive dielectric slabs." Light Propagation in Gain Media (n.d.), 28-62. doi:10.1017/cbo9780511973635.003.

[78] Cazeca, Mario J., XinLi Jiang, Jayant Kumar, and Sukant K. Tripathy. "Epoxy matrix for solid-state dye laser applications." Applied Optics 36, no. 21 (1997), 4965. doi:10.1364/ao.36.004965.

[79] "Scattering in Random Media, General scattering in random media scattering in random media." Formulas of Acoustics, 2008, 238-241. doi:10.1007/978-3-540-76833-3_77.

[80] Costela, A., I. Garcia-Moreno, J. M. Figuera, F. Amat-Guerri, and R. Sastre. "Solid-state dye lasers based on polymers incorporating covalently bonded modified rhodamine 6G." Applied Physics Letters 68, no. 5 (1996), 593-595. doi:10.1063/1.116478.

[81] Lawandy, N. M., R. M. Balachandran, A. S. Gomes, and E. Sauvain. "Laser action in strongly scattering media." Nature 368, no. 6470 (1994), 436-438. doi:10.1038/368436a0.

[82] H. Cao,"Optical Properties of Nanostructured Random Media." Topics in Applied Physics, 2002. doi:10.1007/3-540-44948-5.

[83] Genack, Azriel Z., and Jing Wang. "Modes in Random Media." Frontiers in Optics 2010/Laser Science XXVI, 2010. doi:10.1364/fio.2010.fthg7.

[84] Wiersma, Diederik. "The smallest random laser." Nature 406, no. 6792 (2000), 133-135. doi:10.1038/35018184.

[85] Cao, Hui. "Random Lasers: Development, Features and Applications." Optics and Photonics News 16, no. 1 (2005), 24. doi:10.1364/opn.16.1.000024.

[86] Wiersma, Diederik S., and Ad Lagendijk. "Light diffusion with gain and random lasers." Physical Review E 54, no. 4 (1996), 4256-4265. doi:10.1103/physreve.54.4256.

[87] Nabekawa, Y., Y. Shimizu, and K. Midorikawa. "Ultrabroadband regenerative amplifier with a mirror-less cavity." Summaries of Papers Presented at the Lasers and Electro-Optics. CLEO '02. Technical Diges (n.d.). doi:10.1109/cleo.2002.1034114.

[88] Shang, Zhenzhen, Mingchao Yang, and Luogen Deng. "Low–Threshold and High Intensity Random Lasing Enhanced by MnCl2." Materials 9, no. 9 (2016), 725. doi:10.3390/ma9090725.

[89] Okamoto, Koichi, Isamu Niki, Alexander Shvartser, Yukio Narukawa, Takashi Mukai, and Axel Scherer. "Surface-plasmon-enhanced light emitters based on InGaN quantum wells." Nature Materials 3, no. 9 (2004), 601.

[90] Wiersma, Diederik S., Meint P. Van Albada, and Ad Lagendijk. "Random laser?" Nature 373, no. 6511 (1995), 203-204. doi:10.1038/373203b0.

[91] Carminati, R., and R. Pierrat. "Threshold of random lasers with incoherent feedback." Photonic Metamaterials: From Random to Periodic, 2006. doi:10.1364/meta.2006.thd21.

[92] Pierrat, R., and R. Carminati. "Threshold of random lasers in the incoherent transport regime." Physical Review A 76, no. 2 (2007). doi:10.1103/physreva.76.023821.

[93] Ivanov, V. V. "The mean free path of a photon in a scattering medium." Astrophysics 6, no. 4 (1973), 355-367. doi:10.1007/bf01001630.

[94] Krucinski, Martin. "Printer media path closed loop control." 2009 American Control Conference, 2009. doi:10.1109/acc.2009.5160038.

[95] Berube, David, Christopher Cummings, Michael Cacciatore, DietramScheufele, and Jason Kalin. "Characteristics and classification of nanoparticles: Expert Delphi survey." Nanotoxicology 5, no. 2 (2010), 236-243. doi:10.3109/17435390.2010.521633.

[96] Song, Qinghai, ZhengbinXu, Seung H. Choi, Xuanhao Sun, Shumin Xiao, OzanAkkus, and Young L. Kim. "Detection of nanoscale structural changes in bone using random lasers." Biomedical Optics Express 1, no. 5 (2010), 1401. doi:10.1364/boe.1.001401.

[97] Hadler, Joshua, Edna Tobares, and Marla Dowell. "Random testing reveals excessive power in commercial laser pointers." Journal of Laser Applications 25, no. 3 (2013), 032007. doi:10.2351/1.4798455.

[98] Polson, Randal C., and Z. V. Vardeny. "Random lasing in human tissues." Applied Physics Letters 85, no. 7 (2004), 1289-1291. doi:10.1063/1.1782259.

[99] Balachandran, R. M., and N. M. Lawandy. "Interface reflection effects in photonic paint." Optics Letters 20, no. 11 (1995), 1271. doi:10.1364/ol.20.001271.

[100] LaRochelle, S., P. Mathieu, V. Larochelle, and J. Dubois. "Long range interrogation of laser paints for identification applications." CLEO '97., Summaries of Papers Presented at the Conference on Lasers and Electro-Optics (n.d.). doi:10.1109/cleo.1997.602368.

[101] Yeh, Chien-Hung. "Tunable Dual-Wavelength Laser Scheme by Optical-Injection Fabry-Perot Laser Diode." Semiconductor Laser Diode Technology and Applications, 2012. doi:10.5772/35892.

[102] Tiwari, Jitendra N., Rajanish N. Tiwari, and Kwang S. Kim. "Zero-dimensional, one-dimensional, two-dimensional and three-dimensional nanostructured materials for advanced electrochemical energy devices." Progress in Materials Science 57, no. 4 (2012), 724-803. doi:10.1016/j.pmatsci.2011.08.003.

[103] Gubicza, Jenő. "Defect Structure in Bulk Nanomaterials Processed by Severe Plastic Deformation." Defect Structure and Properties of Nanomaterials, 2017, 59-93. doi:10.1016/b978-0-08-101917-7.00003-7.

[104] Lv, Wei, Patrick E. Phelan, RajasekaranSwaminathan, Todd P. Otanicar, and Robert A. Taylor. "Multifunctional Core-Shell Nanoparticle Suspensions for Efficient Absorption." Journal of Solar Energy Engineering 135, no. 2 (2012). doi:10.1115/1.4007845.

[105] Mélinon, Patrice, Sylvie Begin-Colin, Jean L. Duvail, FabienneGauffre, Nathalie H. Boime, Gilles Ledoux, Jérôme Plain, Peter Reiss, Fabien Silly, and BénédicteWarot-Fonrose. "Engineered inorganic core/shell nanoparticles." Physics Reports 543, no. 3 (2014), 163-197. doi:10.1016/j.physrep.2014.05.003.

[106] Gurunathan S., Han J.W., Kwon D.N., Kim J.H. Enhanced antibacterial and anti-biofilm activities of silver nanoparticles against Gram-negative and Gram-positive bacteria. Nanoscale Res. Lett. 2014;9:373. doi: 10.1186/1556-276X-9-373.

[107] Ekinci, H. H. Solak, and J. F. Löffler , Plasmon resonances of aluminum nanoparticles and nanorods. Journal of Applied Physics 104, 083107 (2008) aip.scitation.org/doi/abs/10.1063/1.2999370

[108] AshishRai, Donggeun Lee, Kihong Park, and Michael R. Zachariah, Importance of Phase Change of Aluminum in Oxidation of Aluminum Nanoparticles. The Journal of Physical Chemistry B 2004 108 (39), 14793-14795 pubs.acs.org/doi/abs/10.1021/jp0373402

[109] Benjamin D. Clark, Christian R. Jacobson, Minhan Lou, David Renard, Gang Wu, Luca Bursi, Arzeena S. Ali, Dayne F. Swearer, Ah-Lim Tsai, Peter Nordlander, and Naomi J. Halas, Aluminum Nanocubes Have Sharp Corners. ACS Nano 2019 13 (8), 9682-9691 pubs.acs.org/doi/abs/10.1021/acsnano.9b05277

[110] Martin, R. C.; Locatelli, E.; Li, Y.; Matteini, P.; Monaco, I.; Cui, G.; Li, S.; Banchelli, M.; Pini, R.; Comes Franchini, M. One-Pot Synthesis of Magnesium Nanoparticles Embedded in a Chitosan Microparticle Matrix: a Highly Biocompatible Tool for in Vivo Cancer Treatment. J. Mater. Chem. B 2016, 4, 207– 211, DOI: 10.1039/C5TB02499D [Crossref], [PubMed], [CAS].

[111] ocatelli, E.; Matteini, P.; Sasdelli, F.; Pucci, A.; Chiariello, M.; Molinari, V.; Pini, R.; Comes Franchini, M. Surface Chemistry and Entrapment of Magnesium Nanoparticles into Polymeric Micelles: a Highly Biocompatible Tool for Photothermal Therapy. Chem. Commun. 2014, 50, 7783–
7786, DOI10.1039/C4CC01513D [Crossref], [PubMed], [CAS.

[112] Sharma, B.; Frontiera, R. R.; Henry, A.-I.; Ringe, E.; Van Duyne, R. P. SERS: Materials, Applications, and the Future. Mater. Today 2012, 15, 16– 25, DOI:10.1016/S1369-7021(12)70017 2 [Crossref] , [CAS].

[113] Hamidi-Asl, Ezat, Freddy Dardenne, SanazPilehvar, Ronny Blust, and Karolien De Wael. "Unique Properties of Core Shell Ag@Au Nanoparticles for the Aptasensing of Bacterial Cells." Chemosensors 4, no. 3 (2016), 16. doi:10.3390/chemosensors4030016.

[114] Qin, Zhenpeng, and John C. Bischof. "Thermophysical and biological responses of gold nanoparticle laser heating." Chem. Soc. Rev 41, no. 3 (2012), 1191-1217. doi:10.1039/c1cs15184c.

[115] Riley, Rachel S., and Emily S. Day. "Gold nanoparticle-mediated photothermal therapy: applications and opportunities for multimodal cancer treatment." Wiley Interdisciplinary Reviews: Nanomedicine and Nanobiotechnology 9, no. 4 (2017), e1449. doi:10.1002/wnan.1449.

[116] Assadi, Zahra, GitiEmtiazi, and Ali Zarrabi. "Hyperbranchedpolyglycerol coated on copper oxide nanoparticles as a novel core-shell nano-carrier hydrophilic drug delivery model." Journal of Molecular Liquids 250 (2018), 375-380. doi:10.1016/j.molliq.2017.12.031.

[117] Campani, Virginia, SimonaGiarra, and Giuseppe De Rosa. "Lipid-based core-shell nanoparticles: Evolution and potentialities in drug delivery." OpenNano 3 (2018), 5-17. doi:10.1016/j.onano.2017.12.001.

[118] Priecel, Peter, Hammed Adekunle Salami, Romen H. Padilla, ZiyiZhong, and Jose A. Lopez-Sanchez. "Anisotropic gold nanoparticles: Preparation and applications in catalysis." Chinese

Journal of Catalysis 37, no. 10 (2016), 1619-1650. doi:10.1016/s1872-2067(16)62475-0.

[119] Choe, Minhyeok, Chu-Young Cho, Jae-Phil Shim, Woojin Park, Sung K. Lim, Woong-Ki Hong, Byoung Hun Lee, Dong-Seon Lee, Seong-Ju Park, and Takhee Lee. "Au nanoparticle-decorated graphene electrodes for GaN-based optoelectronic devices." Applied Physics Letters 101, no. 3 (2012), 031115. doi:10.1063/1.4737637.

[120] Moos, Rafaela, Ismael L. Graff, Vinicius S. De Oliveira, Wido H. Schreiner, and Arandi G. Bezerra. "Influence of plasmon coupling on the photoluminescence of ZnS/Ag nanoparticles obtained by laser irradiation in liquid." Optical Materials 72 (2017), 98-105. doi:10.1016/j.optmat.2017.05.050.

[121] George, J. P., P. F. Smet, J. Botterman, V. Bliznuk, W. Woestenborghs, D. Van Thourhout, K. Neyts, and J. Beeckman. "Lanthanide-Assisted Deposition of Strongly Electro-optic PZT Thin Films on Silicon: Toward Integrated Active Nanophotonic Devices." ACS Applied Materials & Interfaces 7, no. 24 (2015), 13350-13359. doi:10.1021/acsami.5b01781.

[122] Sathish, S., and S. Balakumar. "Effect of synthesis parameters of polyol technique on photoluminescence properties of ZnSe nanoparticles." Journal of Luminescence 190 (2017), 272-278. doi:10.1016/j.jlumin.2017.05.033.

[123] Schinca, D. C., L. B. Scaffardi, F. A. Videla, G. A. Torchia, P. Moreno, and L. Roso. "Silver–silver oxide core–shell nanoparticles by femtosecond laser ablation: core and shell sizing by extinction spectroscopy." Journal of Physics D: Applied Physics 42, no. 21 (2009), 215102. doi:10.1088/0022-3727/42/21/215102.

[124] Chen, Chaonan, Zhewei Wang, Ke Wu, and Hui Ye. "Tunable near-infrared epsilon-near-zero and plasmonic properties of Ag-ITO co-

sputtered composite films." Science and Technology of Advanced Materials 19, no. 1 (2018), 174-184. doi:10.1080/14686996.2018.1432230.

[125] Lysak, Volodymyr V. "Optical properties of core/shell nanoparticles: Comparison of TiO 2 /Ag and Ag/TiO 2 structures." Materials Today: Proceedings 4, no. 3 (2017), 4890-4895. doi:10.1016/j.matpr.2017.04.091.

[126] Hong, Ruijin, Wen Shao, Wenfeng Sun, Cao Deng, Chunxian Tao, and Dawei Zhang. "The influence of dielectric environment on the localized surface plasmon resonance of silver-based composite thin films." Optical Materials 83 (2018), 212-219. doi:1mahe0.1016/j.optmat.2018.06.019.

[127] C. Sönnichsen, ―Plasmons in metal nanostructures,‖ *Dissertation*, vol. 27, no. June, p. 134, 2001, doi: 10.1017/CBO9781107415324.004.

[128] V. G. Kravets, A. V. Kabashin, W. L. Barnes, and A. N. Grigorenko, ―Plasmonic Surface Lattice Resonances: A Review of Properties and Applications,‖ *Chem. Rev.*, vol. 118, no. 12, pp. 5912–5951, 2018,doi: 10.1021/acs.chemrev.8b00243.

[129] J. Liu *et al.*, ―Recent advances of plasmonic nanoparticles and their applications,‖ *Materials (Basel).*, vol. 11, no. 10, 2018, doi: 10.3390/ma11101833.

[130] K. Okamoto, I. Niki, A. Shvartser, Y. Narukawa, T. Mukai, and A. Scherer, ―Surface-plasmon-enhanced light emitters based on InGaN quantum wells,‖ *Nat. Mater.*, vol. 3, no. 9, pp. 601–605, 2004, doi: 10.1038/nmat1198.

[131] O. Popov, A. Zilbershtein, and D. Davidov, ―Random lasing from dye-gold nanoparticles in polymer films: Enhanced gain at the

surface-plasmon-resonance wavelength,‖ *Appl. Phys. Lett.*, vol. 89, no. 19, 2006, doi: 10.1063/1.2364857.

[132] A. Yadav, L. Zhong, J. Sun, L. Jiang, G. J. Cheng, and L. Chi, ―Tunable random lasing behavior in plasmonic nanostructures,‖ *Nano Converg.*, vol. 4, no. 1, pp. 1–8, 2017, doi: 10.1186/s40580-016-0095-5.

[133] C. Noguez, ―Surface plasmons on metal nanoparticles: The influence of shape and physical environment,‖ *J. Phys. Chem. C*, vol. 111, no. 10, pp. 3606–3619, 2007, doi: 10.1021/jp066539m.

[134] P. Taylor and R. G. W. Brown, ―Absorption and Scattering of Light by Small Particles,‖ no. May 2012, 2010.

[135] E. Dulkeith*et al.*, ―Fluorescence Quenching of Dye Molecules near Gold Nanoparticles: Radiative and Nonradiative Effects,‖ *Phys. Rev. Lett.*, vol. 89, no. 20, pp. 12–15, 2002, doi: 10.1103/PhysRevLett.89.203002.

[136] S. Ning*et al.*, ―Enhancement of amplified spontaneous emission in organic gain media by the metallic film,‖ *Org. Electron.*, vol. 15, no. 9, pp. 2052–2058, 2014, doi: 10.1016/j.orgel.2014.05.022.

[137] E. Heydari, R. Flehr, and J. Stumpe, ―Influence of spacer layer on enhancement of nanoplasmon-assisted random lasing,‖ *Appl. Phys. Lett.*, vol. 102, no. 13, 2013, doi: 10.1063/1.4800776.

[138] David Renard, ShuTian, ArashAhmadivand, Christopher J. DeSantis, Benjamin D. Clark, Peter Nordlander, and Naomi J. Halas, Polydopamine-Stabilized Aluminum Nanocrystals: Aqueous Stability and Benzo[a]pyrene Detection. ACS Nano 2019 13 (3), 3117-3124 pubs.acs.org/doi/abs/10.1021/acsnano.8b08445